VIABILITY, DNA DAMAGE, APOPTOSIS, NECROSIS, AND p53 GENE EXPRESSION OF HUMAN CELLS UPON EXPOSURE TO GOLD AND SILVER NANOPARTICLES WITH DIFFERENT SIZE AND SURFACE CHEMISTRY

by

İlknur Sur

Submitted to the Institute of Graduate Studies in
Science and Engineering in partial fulfillment of
the requirements for the degree of
Master of Science
in
Biotechnology

Yeditepe University

2010

VIABILITY, DNA DAMAGE, APOPTOSIS, NECROSIS, AND p53 GENE EXPRESSION OF HUMAN CELLS UPON EXPOSURE TO GOLD AND SILVER NANOPARTICLES WITH DIFFERENT SIZE AND SURFACE CHEMISTRY

APPROVED BY:

Assoc. Prof. Mustafa Culha (Supervisor) .....

Assist. Prof. Dilek Telci .....

Prof. Dr. Bayram Yılmaz .....

DATE OF APPROVAL: 17/08/2010

This thesis is dedicated to my beloved grandmother and mother, Ayşe Sur, Safigülü Sur who always gave the mental support to do the best thing, and always prayed for me.

ACKNOWLEDGEMENTS

First and foremost, I wish to thank to my supervisor, Associate Prof. Dr. Mustafa Çulha, for giving me the valuable opportunity to study in Nanobiotechnology Research Group. He taught me how to become a real scientist and I could not achieve so much today without his supervision.

I would like to thank my graduate committee Asst. Prof. Dr. Dilek Telci, and Prof. Dr. Bayram Yılmaz. I want to give a special thanks to research group of Asst. Prof. Dr. Dilek Telci, especially to Merve Erdem who has always been available for help without hesitation. I also acknowledge Sinem Eyüboğlu for her help with comet assay.

I thank to all members of Nanobiotechnology Research Group namely, Deniz Sandal, Kemal Keseroğlu, İsmail Sayın, Ertuğ Avcı, Melis Uslu, Deniz Saatçi, Seda Demir, Sevcan Ayaksız, Sercan Keskin. I especially thank to Mehmet Kahraman for his help and encouragement. When I joined to the group, he taught me everything and let me acquaint myself with the lab. I would like to also give the special thanks to my lab mate, Mine Altunbek, with for working hand by hand with me during the last year of my study.

Thanksgiving to my almighty God who is the source of my life and my strength. I would like to thank my parents, Safigülü Sur and Rıza Sur, who always love and support me at any time. I thank to my brother, Cihan Sur, and my grandparents Aynur Yılmaz, Ayşe Sur, Mehmet Sur, Mustafa Yılmaz for their prayers. They taught me responsibility, honesty, and dedication and they gave me the most unconditional love that could exist, they always trusted me no matter what. I would like to also thank my relatives, Zeki Sur, Kazım Karataş, Mahmut Demir, and Ali Rıza Karataş for their support and trusting to me. Above all, I would like to thank to my uncles Metin Yılmaz, Ali Sur who have impacted my life for the better.

Finally, I want to express my deepest gratitude to The Scientific and Technical Research Council of Turkiye (TUBİTAK) for financial support during my master education.

ABSTRACT

VIABILITY, DNA DAMAGE, APOPTOSIS, NECROSIS, AND p53 GENE EXPRESSION OF HUMAN CELLS UPON EXPOSURE TO GOLD AND SILVER NANOPARTICLES WITH DIFFERENT SIZE AND SURFACE CHEMISTRY

The interaction of nanoparticles (NPs) with human living cells is of great interest due to their rising use in consumer products and medicine. Among all, gold nanoparticles (AuNPs) and silver nanoparticles (AgNPs) are already in consumer and medical products and their wide spread use seems inevitable due to their unique physicochemical and therapeutic properties. However, there is neither a clear understanding nor a consensus on their possible adverse effect on human health. Therefore, there must be more studies devoted for in depth understanding of their mode of interactions with the living systems. The present thesis aims to provide a systematic approach to investigate the influence of size, surface chemistry, and dose of AuNPs and AgNPs on the cell viability, cellular DNA damage, p53 gene expression, apoptosis and necrosis mechanisms. The cellular response to two different sizes of AuNPs and AgNPs with different surface chemistry was evaluated in two human cell lines, primary human dermal fibroblast isolated from human foreskin and A549 lung cancer cells.

The results demonstrated that 13 nm and 50 nm AuNPs did not cause considerable cell death and cellular DNA damage, whereas 7 nm and 29 nm AgNPs showed pronounced cytotoxic and genotoxic effects for both cells at the concentration of 25.0 $\mu g\ ml^{-1}$. The results from this study also suggest that the small size NPs caused more cytotoxicity and genotoxicity. Although all the NPs without lactose or oligonucleotide modified AgNPs caused high levels of necrosis in the human dermal fibroblasts, the necrosis remained at low levels in A549 cells. Notably, the lactose modified AgNPs caused significant cell death, cellular DNA damage, apoptosis, and p53 expression in A549 cells while the degree of these effects was found to be low in the human dermal fibroblast cells. The specificity of lactose modified AgNPs induced apoptosis in the A549 cells implies that these NPs could be replaced with AuNPs in applications to kill cancer cells by using photothermal therapy.

Furthermore, the 50 nm AgNPs should be injected directly into the tumor due to adverse effects on both human cells.

ÖZET

İNSAN HÜCRELERİNİN FARKLI BÜYÜKLÜKTE VE YÜZEY KİMYASINA SAHİP ALTIN VE GÜMÜŞ NANOPARÇACIKLARA MARUZ KALMASI SONUCU CANLILIĞI, DNA HASARI, APOPTOZU, NEKROZU VE p53 GEN EKSPRESYONU

Nanoparçacıkların tüketici ürünlerinde ve tıpta artan kullanımından dolayı canlı hücrelerle olan ilişkileri ilgi odağı olmaktadır. Nanoparçacıklar arasından, altın ve gümüş nanoparçacıklar tüketici ve tıbbi ürünlerde kullanılmakta ve fizikokimyasal ve terapatik özelliklerinden dolayı yaygın kullanımları kaçınılmaz görülmektedir. Bununla birlikte, nanoparçacıkların insan sağlığına olabilecek kötü etkileri üzerine ne açık bir fikir ne de ortak bir görüş vardır. Bundan dolayı, nanoparçacıkların canlı sistemlerle olan ilişki durumlarını derinlemesine anlamak için daha fazla çalışma yapılmadır. Bu tez, altın ve gümüş nanoparçacıkların büyüklüğünün, yüzey kimyasının ve konsantrasyonunun hücre yaşamı, hücresel DNA hasarı, p53 gen ekspresyonu, apoptoz ve nekroz mekanizmaları üzerine etkisini araştırmak için sistematik bir yaklaşım sağlamayı amaçlamaktadır. Farklı yüzey kimyasına sahip, iki farklı büyüklükteki altın ve gümüş nanoparçacıklara olan hücresel cevap iki insan hücresinde; insan sünnet derisinden izole edilmiş primer insan dermal fibroblast ve A549 akciğer kanseri hücrelerinde, değerlendirilmiştir.

Bu sonuçlar, iki hücre için 25.0 μg ml^{-1} konsantrasyonundaki 13 nm ve 50 nm altın nanoparçacıkların ciddi hücre ölümü ve hücresel DNA hasarına sebep olmadığını, 7 nm ve 29 nm gümüş nanoparçacıkların ise önemli sitotoksik ve genotoksik etki gösterdiğini ortaya koymuştur. Bu çalışmanın sonuçları ayrıca, küçük büyüklükteki nanoparçacıkların daha fazla sitotoksisite ve genotoksisiteye yol açtığını göstermiştir. İnsan dermal fibroblast hücrelerinde laktoz ve oligonükleotid modifiyeli gümüş nanoparçacıklar dışındaki tüm nanoparçacıklar yüksek derecede nekroza sebep olurken, A549 hücrelerinde nekroz düşük seviyede kalmıştır. Dikkat çekecek şekilde, laktoz modifiyeli gümüş nanoparçacıklar A549 hücrelerinde kayda değer seviyede hücre ölümü, hücresel DNA hasarı, apoptoz, ve p53 gene ekspresyonuna yol açarken, insan dermal fibroblast hücrelerinde bu etkilerin derecesi düşük bulunmuştur. Laktoz modifiyeli gümüş nanoparçacıkların A549 hücrelerindeki hücre ölümünü uyarma özelliği, bu nanoparçacıkların fototermal terapi kullanılarak kanser

hücrelerinin öldürüldüğü uygulamalarda altın nanoparçacıkların yerini alabileceğini vurgulamıştır. Buna ek olarak, iki insan hücresine olan olumsuz etkilerinden dolayı, 50 nm gümüş nanoparçacıklar direkt olarak tümöre enjekte edilebilir.

TABLE OF CONTENTS

LIST OF FIGURES

LIST OF TABLES

LIST OF SYMBOLS / ABBREVIATIONS

d.nm	diameter in nanometer scale
kDa	kilo Dalton
min	minute
nm	nanometer

AFM	Atomic Force Microscopy
AgNPs	Silver nanoparticles
AuNPs	Gold nanoparticles
CNT	Carbon nanotube
DNA	Deoxyribonucleic acid
DLS	Dynamic Light Scattering
DMEM	Dulbecco's Modified Eagle's Medium
MNP	Magnetic nanoparticle
NIR	Near Infrared Region
NPs	Nanoparticles
NMs	Nanomaterials
QD	Quantum dot
PBS	Phosphate Buffered Saline
RNA	Ribonucleic acid
SEM	Scanning Electron Microscopy
SERS	Surface enhanced raman spectroscopy
ssDNA	Single-stranded deoxyribonucleic acid
TEM	Transmission Electron Microscopy
UV/Vis	Ultraviolet/Visible

1. INTRODUCTION

In today's technological world, nanotechnology is becoming the fastest growing area of scientific research and has a wide range of applications. Nanotechnology is central to many of the most revolutionary techniques for the fabrication of products ranging from consumer items and electronics to biomedical devices. The use of nanomaterials (NMs) in biomedical applications is one of the promising directions that nanotechnology is taking at this time [1].

With the enormous developments in nanotechnology, NMs provide a good potential for their use in many commercially available products like sunscreens and cosmetics, pharmaceuticals stain resistant clothing and sport equipment, automobile catalytic converters, dental bonding agent, cleaning products, and burn and wound dressing, but many are the fields of possible future applications of nanotechnology in drug delivery systems, energy, nanomedicine, environmental remediation, and material applications [2] The need to improve NMs for medical applications has generated interest in the development of multifunctional nanomaterial devices [3].

NPs are typically in the range of 1 to 100 nm in size, comparable to large biological molecules such as enzymes, receptors, and antibodies. Utilizing NPs has opened the doors for cancer diagnostics, therapeutics and drug delivery [4-6]. On the account of their highly fluorescent features, NPs can be used to label cancer cell markers [7]. For this reason, NP-cancer cell interactions have become a significant part of nanobiotechnology and nanotoxicology.

Among the various NPs, metal NPs have attracted a tremendous attention because of the potential for developing assays in the fields of medical sciences and pharmacology [8,9]. The most interesting chemical elements used as NPs for medical applications are AuNPs and AgNPs [10,11]

Due to their unique physicochemical properties and ability to function at the cellular and molecular level of biological interactions, AuNPs are being actively investigated as the

next generation of therapeutic agents [12] and as vehicles for targeted drug delivery [9]. The AuNPs are explained as nontoxic or toxic depending on the size, dose, and surface functionalization. Earlier studies indicated that exposure to AuNPs did not cause any adverse effects on mammalian cells [13]. On the contrary, Yen et al. claimed that the AuNPs showed size and concentration dependent toxicity [14]. They demonstrated that the smaller AuNPs caused a greater toxic effect in murine macrophages than the larger AuNPs caused. Another significant study confirmed that the 20 nm AuNPs treated human embryonic lung fibroblasts down regulated the cell cycle and DNA repair genes thereby causing cell death [15]. Due to light-absorbing properties of AuNPs, gold-silica nanoshells are used in the nanoshell-assisted photothermal therapy (NAPT) to destruct cancerous cells by using near infrared region (NIR) light [16]. With a wide range of applications in the detection, diagnosis, and treatment of illnesses, AuNPs may soon play an important role in meeting the healthcare needs of tomorrow.

Among all the NMs in consumer products, the use of AgNPs has the highest degree of commercialization and they are widely used in many consumer products as the biocidal agent. Especially since the significance of AgNPs increases in medicine, the exposure of the human body to AgNPs increases and the consequent toxicological effects become more important. The study by Carlson et al. showed that the different size of AgNPs may induce cytotoxicity via the apoptosis and necrosis mechanisms depending on the exposed dose and sizes on different cells [17]. Studies from Kawata and coworkers showed an upregulation of DNA repair-associated genes in hepatoma cells treated with the low concentration of AgNPs, proposing possible DNA damaging effects [18]. On a similar note, Ahamed et al. demonstrated that the surface chemistry of AgNPs could also be important for the cytotoxicity and genotoxicity in cells [19]. In the terms of the wound healing, the use of AgNPs had direct anti-inflammatory effects and improved the process significantly when compared with the controls [20]. Another important point of using AgNPs in living cells is cellular imaging because of their good fluorescence enhancement properties as a result of their plasmonic properties, which can be easily tuned for absorption band from visible to NIR region. Moreover, the AgNPs can also be an attractive alternative to AuNPs for the surface-enhanced Raman scattering (SERS) applications [21-23].

In this study, we specifically explored the question of size and surface chemistry on the balance between toxicity and p53 gene related mechanisms. In light of the potential exposure and medical applications of NPs, a healthy human primary cell line and cancer cell line have been chosen to evaluate the potential cell interaction of these NPs. The effect of NPs on human dermal fibroblasts was chosen since one of the major routes to exposure to NPs is though skin. The systematic study of the influence of size and surface chemistry was performed to understand the cytotoxicity, cellular DNA damage, apoptosis and necrosis, p53 gene expression in human cell lines. The living cells internalized the NPs and upregulated p53 gene expression due to cellular DNA damage. The prime cause of the cell death is considered as apoptosis or necrosis of these cells following the NP treatment. Gene expression study indicated a robust upregulation of p53 gene after 6 h incubation with a 25.0 μg ml^{-1} NPs. The 7 nm and 29 nm AgNPs caused cell death associated with the cellular DNA damage while 50 nm AgNPs induced p53 expression followed by apoptosis in A549 cells.

2. THEORETICAL BACKGROUND

2.1. INTERACTION OF LIGHT WITH NOBLE METAL NPs

For a better understanding of the applications of noble metal NPs, it is important to understand the fundamentals behind their unusual optical properties. Therefore, a brief discussion of interaction of light with noble metal NPs is first introduced here followed by their applications.

The attractive optical properties of noble metal particles such as AuNPs and AgNPs lead the increasing interest for their applications in biomedical sciences [24]. Plasmonics is an area that explores the interactions of light with metals [25-27]. When the AuNPs and AgNPs interact with ordinary white light, they absorb and scatter the light ($C_{ext} = C_{abs} + C_{sca}$) at the same time. The absorbed light not only excites the surface plasmons but also is converted to heat [25]. The photons converted to heat can be used as local heater where they reside. The scattered photons by NPs can be used for cellular and biomedical imaging. More recently, AuNPs were used as specialized microscopic probes to study cancer cells, because AuNPs selectively accumulate in tumor cells and visualized as showing bright spots using an ordinary light microscope [28,29]. El Sayed and his colleagues found that the EGFR conjugated AuNPs have been used to detect cancer cells by exploiting the light-scattering properties of Au nanoconjugates and this model was offered as a selective technique in molecularly targeted photothermal therapy in vivo using a continuous wave laser at low powers [30]. When the potentials of AuNPs and AgNPs are considered, they could be a medical boon for treatment and prevention of cancer disease. Furthermore, the AuNPs and AgNPs could be major class of NMs with the potential to develop current clinical diagnostic and therapeutic techniques for other diseases.

2.2. INTERACTION OF NANOPARTICLES WITH CELLS

NPs can be used in useful applications but research has also revealed that NPs may also cause adverse effects in living cells systems. Therefore, their possible effects must be investigated starting from basic units of life. Healthy human cell lines, such as human

dermal fibroblast cells, are the most sensitive and delicate cells in bioorganisms, and are responsible for being the source of collagen and elastin of the extracellular matrix. One of the great concerns in science and technological development in the twenty-first century is that NPs may produce adverse effects on function and viability of human dermal fibroblast cells owing to their ability to pass through the biological membranes [14].

At the cellular level some important insights have come from studies on cellular response to AuNPs and AgNPs [31,32]. Because of its chemical inertness, Au has been used internally in humans for the past 50 years, from its use in teeth to implants to radioactive gold used in cancer treatment [33,34]. Exposure to NPs (such as AuNPs and AgNPs) of the healthy human cells is also becoming increasingly widespread through antibacterial fabrics and coatings. However, effects of the presence of metal NPs in the skin and through the membrane have not yet been fully investigated. The NPs have better mobility and it is anticipated that the transportation of NPs across the membrane is possible by the pinocytosis and receptor-mediated endocytosis [35,36]. Furthermore, the NPs may be taken up directly into the human dermal fibroblast cells by the endocytosis [37]. Perdonet et al. reported that NPs exposure can induce impairments to human dermal fibroblast cells [38].

Apart from healthy cells, the use of the cancer cells is one of the promising modality for cancer cell-NPs based therapy applications. Cancer develops when the DNA of a normal cell gets changed or mutated. By the time, DNA of living cell gets damaged, either the cell may repair it or the cell may die. As a result of unrepaired DNA, it triggers cancer initiation in living cells [39]. For human beings, cancer caused a lot of deaths and one of the most leading causes of cancer mortality in the worldwide is lung cancer with almost one million cases every year [40]. In the lung cancer cells, A549 lung cancer line is a cellular model for lung cancer studies with thousands of publications within many different scientific areas. Many researches have shown that NPs had different effects on A549 cells. Studies from Bhattacharya and coworkers demonstrated that the titanium dioxide NPs have been shown to induce oxidative stress in A549 and BEAS-2B lung cell lines [41]. The study by Uboldi et al. showed that the treatment of the A549 cells to the AuNPs caused cell death due to excess of sodium citrate [42]. Furthermore, the AgNPs caused to increase ROS production, apoptotic and necrotic cell death in the A549 cells [43].

2.3. CYTOTOXICITY OF NANOPARTICLES

Over the years, a plethora of different assays for cytotoxicity has been developed that detects cell viability. Most of the times, NPs have effects on the cell viability that can be detected by the MTS assay, which possess the advantage of being suitable for detection of cytotoxicity in cell cultures. The MTS method is a standard colorimetric assay that measures the activity of enzymes in mitochondria. The MTS tetrazolium compound is reduced to formazan in the mitochondria of living cells, changing from yellow to purple. By NADPH or NADH produced by dehydrogenase enzymes in metabolically active cells, the conversion is accomplished [44]. The quantity of formazan product is measured by the absorbance at 490 nm which is directly proportional to the number of living cells.

The cytotoxicity studies of AuNPs and AgNPs on human healthy cells is crucial due to the fact that these NPs are commonly used in consumer products, medical world. There are various reports, which describe these NPs as cytotoxic [45] or non-toxic [10] because of their surface chemistry and size. Pernodet et al. reported that gold/citrate NPs impaired the cell viability of human dermal fibroblasts and induced an abnormal formation of actin filaments, causing therefore a reduced cellular motility and influencing the cell morphology [38].

As stated earlier, although the NPs need to be biocompatible and nontoxic for the therapeutic applications, the NPs can bring cytotoxic effects depending on their concentration, size, shape, and surface modification in the lung cancer cells [43]. In a study by Patra et al. showed that citrate-capped AuNPs are caused cell death response in A549 cells whereas no cytotoxicity was seen in BHK21 (hamster kidney) or HepG2 (human hepatocellular liver carcinoma) cells [45]. A recent work by Foldbjerg and his coworkers assessed the toxicity of AgNPs by MTT assay and reported that the AgNPs had adverse effects on A549 cell viability [43]. Further research is needed to elucidate the biological impact of noble metal NPs on the human cells.

2.4. CELLULAR DNA DAMAGE EFFECT OF NANOPARTICLES

To find out if a material is genotoxic or not, a genotoxicity assay must be performed. The genotoxicity assays are rapid, standardized, sensitive, and inexpensive means for determining whether a material contains significant biologically harmful effects or not. There are different methods to determine genotoxicity, such as comet assay. This method is a determination of DNA damage in vivo and in vitro has been highlighted in many studies [46,47]. Undamaged cells will have intact nucleotides and damaged cells will appear as comets with a head and tail. The detected level of tail momentum is proportional to the amount of DNA damage. Numerous studies have used the Comet assay to assess DNA damage upon NPs treatment [48-51].

Especially since the significance of AuNPs and AgNPs increases in medicine, the consequent genotoxicological effects become important. Besides, the surface chemistry or modification of NPs is important for genotoxicity in cells so that we need to not only decrease but also improve their toxicity in various cells with chemical surface modifications because the NPs have some ideal characteristics on the account of cellular studies [52]. Furthermore, since there is a close relationship between DNA damage and cancer, the NPs that are potent in leading cellular DNA damage can be considered as more likely to have an effect on cancer formation.

In human dermal fibroblast cells, cerium dioxide NPs showed genotoxic effects at very low doses [53]. For A549 cells, the genotoxicity study by Karlssonn et al. suggested that the CuO NPs showed the most adverse effect on cell viability as well as DNA damage. The ZnO NPs had cytotoxic and genotoxic effects but the TiO_2 NPs only caused DNA damage. They also found that at the lowest dose of carbon nanotubes (CNTs) had the cytotoxic effects and caused DNA damage [48].

2.5. EFFECTS OF NPs ON CELL APOPTOSIS AND NECROSIS

The term “apoptosis” is defined as organized, energy dependent process of programmed cell death and it plays a significant role in the maintenance of normal cellular homeostasis by removing the damaged cells [54]. When cells are in senescence or

threatened by the environment, they commit suicide by activating a signaling cascade that ends in apoptosis. The process of apoptosis is characterized by shrinking, condensing and death of cells without damaging their neighbors. Furthermore, the cytoskeleton collapses, the nuclear envelope disassembles and the nuclear DNA breaks up into fragments [55]. In addition, apoptosis involves many pathways that include the activation of several proteins. The caspases and p53 protein has a crucial role in inducing apoptosis.

Apoptosis has different characteristics that can be used to detect apoptotic activity within cells. Externalization of phosphatidylserine is one of the most reliable methods to detect apoptosis. The assays include is Annexin V Conjugate that detects, an indicator of intermediate stages of apoptosis. The apoptosis test performed in this research is Annexin-V FITC apoptosis detection assay which is capable of staining cells during apoptosis by detecting the loss of asymmetry in cell membrane.

Necrosis or pathologic cell death can either result from outer physical actions or severe cellular damage induced by chemical processes [55]. In necrosis, the cell swells and bursts, loses integrity of mitochondrial, lysosomal and plasma membranes, releases of its contents into surrounding area causing inflammation. Since necrosis occurs when cell membrane is damaged chemically or physically, it could be a possible cell death mechanism after NPs exposure.

The study of necrosis of AuNPs by Pan et al. demonstrated that 1.4 nm AuNPs triggered necrosis by mitochondrial damage and oxidative stress [56]. One of the most important findings by El Sayed et al. has been demonstrated that nuclear targeting of AuNPs in cancer cells cause cytokinesis arrest prevents to complete cell division and leads to apoptosis [57]. Several studies have demonstrated that the AgNPs significantly induced cell apoptosis or necrosis in different cell types [57,58]. In a similar study, the apoptotic effect of the AgNPs was reported using mouse NIH3T 3 cells [59]. Foldbjerg et al. noted that the AgNPs exposed A549 cells showed a dose dependent increase in apoptotic and necrotic cells [43]. In addition, the TiO_2 NPs exposed mouse fibroblast cells (L929) were directly necrosed [60].

2.6. EFFECTS OF NPs ON p53 GENE AND PROTEİN EXPRESSION

The p53 gene is considered as the master guardian or molecular policeman of the cell and is involved in major cell cycle checkpoints, DNA repair and apoptotic response to maintain genetic stability [61]. p53 is the most significant gene involved in cancer in humans; it is regarded as a tumor suppressor gene and is mutated in about half of all human cancers [62].

If healthy living cells are deprived of oxygen or exposed to treatments that damage DNA, they increase their p53 protein level and activation in order to suppress the formation of tumors by arresting the cell cycle or by committing cells to apoptosis [63]. In the presence of DNA damage, p53 increases and triggers cell cycle arrest to provide time for the damage to be repaired based on the degree of DNA damage. When the amount of DNA damage is too severe to be repaired, p53 causes self-mediated cell death or apoptosis [64]. Most of the time, the loss of p53 function in cancer cells is dangerous because it allows faulty mutant cells to maintain through the cell cycle and allows them to escape from the apoptosis [63].

The interaction of genotoxic or nongenotoxic agents with cancer cells to reactivate p53 function is under intense investigations due to their possible solutions to prevent cancer [65-68]. Based on an understanding of the normal p53-mediated pathway for suppressing cancer induction, treating the cancer cells with NPs for reactivating p53 has been suggested. Interestingly in the study of Ahamed et al., the copper oxide NPs upregulated the cell cycle checkpoint protein p53 and DNA damage repair proteins Rad51 and MSH2 expression for A549 cells [69]. More recently, Zhu et al. demonstrated that carbon nanotubes accumulate in mouse embryonic stem cells (mESCs) activating the tumor suppressor protein p53 within 2 h of exposure and consequently leading to cellular apoptosis [70]. In a somewhat related, but independent study, Asharani et al. suggested that platinum NPs toxicity showed an increase in DNA damage with down regulation of p53, p21 and cell cycle arrest at the S-phase [71].

3. MATERIALS

The materials used in this study were purchased from diverse suppliers as shown in Table 3.1-3.6.

3.1. CHEMICALS

All chemicals were used as received and H_2O was obtained from Ultrapure Water System (Sartorius, Germany). The cell culture media were purchased from Sigma (Germany).

Table 3.1. Overview of used chemicals

Name	**Supplier**
Acrylamide/Bisacrylamide 30% solution	Sigma, Germany
APS (ammoniumpersulfate)	Sigma, Germany
DMSO	Amresco, UK
EDTA	Sigma, Germany
Gold nitrate	Sigma, Germany
High Melting Agarose	Sigma, Germany
Lactose	Merck, Germany
L-Glutamine	Gibco, UK
Low melting agarose	Sigma, Germany
PBS (phosphate buffered saline)	Gibco, UK
Penicillin/Streptomycin	Gibco, UK
Rainbow molecular weight marker	Amersham Biosciences, USA
RIPA buffer	Santa Cruz Biotechnology, USA
SDS	Sigma, Germany
Silver nitrate	Fluka, Germany
Sodium citrate	Merck, USA
SYBR Green Dye	Sigma, Germany
TEMED	Sigma, Germany
Trypsin-EDTA	Gibco, USA

3.2. ANTIBODIES

Table 3.2. Overview of applied antibodies used in western blotting

Name	Type of Antibody	Supplier
P53 mouse monoclonal antibody	Primary antibody	Santa Cruz Biotechnology, USA
Alfa tubulin mouse monoclonal antibody	Primary antibody	Santa Cruz Biotechnology, USA
Antimouse IgG peroxidase conjugate	Secondary antibody	Sigma, Germany

3.3. KITS

Table 3.3. Overview of used kits

Name	Supplier
Annexin-V FITC apoptosis detection kit	Sigma, Germany
CellTiter96 Aqueous One Solution	Promega, UK
ECL Advance Western Blotting Detection Kit	Amersham, UK
RNA isolation kit	Roche, Germany
Senscript reverse transcriptase	Qiagen, Germany
SYBR Green Master Mix	Qiagen, Germany
Annexin-V FITC apoptosis detection kit	Sigma, Germany

3.4. OLIGONUCLEOTIDES

Table 3.4. The properties of oligonucleotides used in the study

Name	**(5'- 3')**	**Source**
Thiloted oligonucleotides	HS-$(CH_2)_6$AGAGTTCGAAGC	Operon, USA
P53 Sense	CCTTCCCAGAAAACCTACCA	Operon, USA
P53 Antisense	TCATAGGGCACCACCACACT	Operon, USA
β-actin Sense	TCCTGTGGCATCCACGAAACT	Operon, USA
β-actin Antisense	GGAGCAATGATCCTGATCTTC	Operon, USA

3.5. MATERIALS

All of the equipments used for Western blotting were performed using Mini-Protean Tetra Cell and Mini Trans-Blot Module (Bio-Rad Laboratories, USA).

Table 3.5. Overview of used materials

Name	**Supplier**
Coverslips (24x60)	Sail, China
6-12-96 well plates	TPP, Switzerland
Falcon tubes (15 ml, 50 ml)	TPP, Switzerland
PVDF membrane	Roche, Germany
Microscope Slides	Menzel, Germany
Sealing Film, Real Time PCR, UC-500	Axygen, USA
Slide-A-Lyzer Dialysis Cassettes	Thermo Fisher Scientific, Illinois, USA
Tissue culture flasks (25 cm^2, 75 cm^2)	TPP, Switzerland
3MM Whatman paper	Biorad, USA
96 Well PCR Microplate PCR-96-FLT-C	Axygen, USA

3.6. DEVICES

Table 3.6. Overview of used devices

Name	**Supplier**
Bio-Rad iCycler Real-Time PCR system	MJ Research, USA
Centrifuges	Hehich, Germany
ELx800 Absorbance Microplate Reader	Biotek, USA
FACSCalibur flow cytometry system	BectonDickinson, USA
Fluorescence microscopy	Nikon, USA
Gel electrophoresis device	BioRad, Germany
CO_2 Incubator	Nuarre, Germany
Inverted light microscope	Nikon Eclipse TS100, USA
Leica Confocal Microscopy	Leica TCS SP2, Heidelberg, Germany
Nanophotometer	Implen, USA
pH meter	Mettler-Toledo, Germany
SEM	Karl Zeiss EVO 40 model, Germany
TEM	Oxford Instruments, USA
Zetasizer Nano ZS instrument	Malvern, USA

4. METHODS

4.1. SYNTHESIS OF NANOPARTICLES

For the synthesis of AuNPs with different size, sodium citrate was used to act as a reductant but solely as a stabilizer due to its chemical structure as seen in Figure 4.1a.

4.1.1. Synthesis of AuNPs with Sodium Citrate in Different Sizes

4.1.1.1. Synthesis of 13 nm AuNPs

AuNPs were prepared by reduction of $HAuCl_4 \cdot 3H_2O$ with sodium citrate [72]. This procedure generates an average size of 13 nm AuNPs that are well characterized in the literature. Briefly, a 10 ml of 38.8 mM (0.1141 g trisodium citrate in 10 mL water) citrate stock solution was added into 100 ml, 1Mm of $HAuCl_4 \cdot 3H_2O$ solution quickly. The $HAuCl_4 \cdot 3H_2O$ solution was heated until to boil, and then the citrate solution was added into the boiling solution and the solution colour changes from yellow to black and to deep red. The final solution was kept boiling for 15min.

4.1.1.2. Synthesis of 50 nm AuNPs

The 50 nm AuNPs were synthesized by reduction of $HAuCl_4 \cdot 3H_2O$ with sodium citrate [72]. Briefly, a 4 ml of 38,8 mM citrate stock solution was added into 500 ml, 1 mM of $HAuCl_4 \cdot 3H_2O$ solution. The $HAuCl_4 \cdot 3H_2O$ solution was heated until to boil, and then the citrate solution was added into the boiling solution. After the colour changed, the solution is refluxed for an additional 15 min, then the heater is turned off and the solution is stirred until it reached cool to room temperature. The NPs made in this method typically have average size around 50 nm.

4.1.2. Synthesis of AgNPs with Gallic Acid in Different Sizes

For the preparation of AgNPs two stabilizing agents, gallic acid and sodium citrate were used in this work. In the first part, the gallic acid was used as a stabilizer as well as a reducing agent with involving –OH groups, and keeps the prepared particles stable because

of its molecular structure as seen in Figure 4.1 b. The two sizes of AgNPs are synthesized according the method described by Martínez-Castañón et al [73].

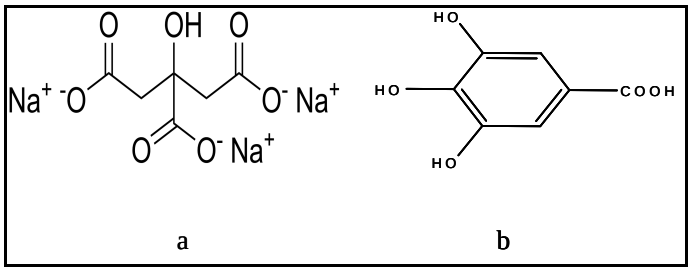

Figure 4.1. The molecular structure of trisodiumcitrate (a) and gallic acid (b)

4.1.2.1. Synthesis of 7 nm AgNPs

A total of 100 mL of $AgNO_3$ 0.001 M was placed in a 250-mL reaction vessel. Under magnetic stirring, 10 mL of deionized water containing 0.01 g of gallic acid was added to the Ag^+ solution. After the addition of gallic acid, the pH value of the solution was immediately adjusted to 11 using a 1.0 M solution of NaOH.

4.1.2.2. Synthesis of 29 nm AgNPs

A total of 0.0169 g of $AgNO_3$ was dissolved in 100 mL of deionized water and this solution was placed in a 250-mL reaction vessel. A total of 0.01 g of gallic acid was dissolved in 10 mL of deionized water and under magnetic stirring were added to the Ag^+ solution. After the addition of gallic acid, the pH value of the solution was immediately adjusted to 10 using a 7.7 M solution of NH_4OH.

4.1.3. Synthesis of AgNPs with Sodium Citrate in Different Sizes

In the second part, the sodium citrate was used for the synthesis of AgNPs. The two sizes of AgNPs are prepared according the method described by Lee-Meisel [73].

4.1.3.1. Synthesis of 20 nm AgNPs

The silver colloid was prepared by using Lee-Meisel method [74]. All solutions of reacting materials were prepared in distilled water. In typical experiment 500 ml of 0.001

M $AgNO_3$ was heated to boiling. To this solution 50 ml of 1% trisodium citrate was added drop by drop. During the process solution was mixed vigorously and solution was heated until colour's change is evident (pale yellow). Then it was removed from the heating element and stirred until cooled to room temperature.

4.1.3.2. Synthesis of 50 nm AgNPs

50 nm AgNPs were synthesized in accordance with Lee-Meisel method [74]. According to this method, $AgNO_3$ (90 mg) was dissolved in distilled water (500 ml). The solution was heated until boiling and added 1% of trisodium citrate solution (10 ml). The mixed solution was boiled during one hour. The solution colour was turned to grayish.

4.1.4. Synthesis of Modified AgNPs

The modified AgNPs are synthesized according to Culha et al. [75]. Briefly, the AgNPs were prepared via the reduction of silver nitrate with sodium citrate reported by Lee and Meisel [74]. The thiol modified lactose solution was diluted 100 times with distilled water. From the diluted solution, a 1.0 µl of lactose derivative was added into 1 mL of the AgNPs suspension. For the attachment of oligonucleotide, an 8 µl of 100 µM thiolated oligonucleotide (5'-HS-$(CH_2)_6$-AGAGTTCGAAGC-3') was added into 1 mL AgNPs suspension and then the modified AgNPs were stirred for 24 h at 20 °C.

To remove uncoupled citrate ion, gallic acid, lactose or ssDNA, the suspensions were dialyzed three times against water at 4 °C by using a Slide-A-Lyzer dialysis cassette with a molecular weight cut-off membrane of 10 kDa. UV-visible spectroscopy, zetasizer, transmission electron microscopy (TEM) and scanning electron microscopy (SEM) were used to characterize the synthesized NPs.

4.2. NANOPARTICLE CHARACTERIZATION ANALYSIS

4.2.1. Dynamic Light Scattering Analysis

All size distribution and zeta potential measurements were performed using a Malvern Zetasizer Nano ZS instrument at 25 °C at 173° scattering angle with a 4 mW He–

Ne laser. The samples of NPs were placed in standard Malvern zeta potential disposable capillary cells and polystyrene cuvettes for zeta potential and size measurements, respectively. The refractive index and absorption of the colloidal suspension were assumed as 2.0 and 0.320, respectively. All measurements were repeated three times.

4.2.2. Transmission Electron Microscopy Analysis

High resolution TEM measurements were performed on JEOL-2100 HRTEM operating at 200 kV (LaB_6 filament) and equipped with an Oxford Instruments 6498 EDS system. The carbon support film coated copper TEM grids were used to analyze samples after locating a very small drop of samples onto them.

4.2.3. Scanning Electron Microscopy Analysis

The characterization of the prepared substrates was performed with a Karl Zeiss EVO 40 model SEM instrument. The accelerating voltage was 156 kV for experiments.

4.3. CELL CULTURE AND NANOPARTICLE TREATMENT

The human dermal fibroblast cells and human lung cancer cells (A549) were used for all experiments. The human dermal fibroblast cell lines were cultured in high-glucose Dulbecco's modified Eagle's medium containing 10% fetal bovine serum (FBS), 100 units/ml penicillin, 100.0 mg/ml streptomycin, 2 mM L-glutamine. The A549 cell lines were grown in DMEM Nutrient Mixture F-12 HAM supplemented with 10% FBS, 100 units/ml penicillin, 100.0 mg/ml streptomycin, 2 mM L-glutamine. Both cell lines were cultured at 37 °C and under 5% CO_2 conditions.

The model cells were used for the in vitro study of the nanoparticle toxicology and p53 gene related mechanisms. At day one, 1.0×10^6 cells were placed in each well of a six-well plate in 1 ml of medium and cultured for 24 h at 37 °C. After 24 h of culture, the medium was changed to fresh medium containing NPs at final concentrations of 12.5, 25.0, 50.0 and 100.0 $\mu g\ mL^{-1}$. The control samples were not treated by any NPs.

4.3.1. MTS Assay

The cytotoxicity induced by NPs on human dermal fibroblast and A549 cells was measured by the MTS-assay according to the manufacturer's instructions. MTS (3-(4,5-dimethyl-thiazol-2-yl)-5-(3-carboxy-methoxy-phenyl)-2-(4-sulfo-phenyl)-2H-tetrazolium) is a tetrazolium-saltbased colorimetric assay for detecting the activity of enzymes (mostly in the mitochondria) that reduce MTS to formazan, giving a purple colour. The cells were seeded in 96-well plates at 3 x 10^3 cells per well. After 24 h incubation period at 37 °C, the cells were treated with 12.5-25.0-50.0-100.0 µg mL^{-1} NPs for 24 h, 48 h and 72 h periods. After removal of medium including NPs, the cells were incubated in the medium containing 10% MTS solution for 3 h. The untreated cells are used as a positive control, and all values from the experiment are correlated with this set of data. The results are displayed as percentage of viable cells compared with the control. The viability was tested at 490 nm using the automated plate reader (KC junior software, Elx80).

4.3.2. Alkaline Single-Cell Gel Electrophoresis

Alkaline single cell gel electrophoresis (Comet assay) detects DNA damage through electrophoresis [76] and subsequent staining in SYBR green dye. At each time point, the cells were washed three times with PBS to remove the residue of NPs in the medium before the cells were detached by trypsin. After that, the cells were centrifuged, resuspended in 1 mL of medium. The cells were embedded in 1% low melting agarose on comet slides and lysed in prechilled lysis solution (2.5 M NaCl, 0.1 M EDTA, 10 mM Tris base, pH 10) with 1% Triton X, 10% DMSO for 1 h at 4 °C. The cells were then subjected to denaturation in alkaline buffer (0.3 M NaCl, 1mM EDTA) for 40 min in the dark at room temperature. Electrophoresis was performed at 25 V and 300 mA for 20 min. The slides were immersed in neutralization buffer (0.5 M Tris-HCl, pH 7.5) for 15 min. The slides were air-dried and stained with SYBR green dye. The tail moments of the nucleus were measured as a function of DNA damage. Hydrogen peroxide was used as positive control. The data was also analyzed in terms of percentage distribution of cells on the basis of tail momentum. Analysis was done using Comet Image Analysis (Comet III) and 50 comets were analyzed per concentration.

4.3.3. Annexin-V Staining

To distinguish apoptotic from necrotic cell death induced by NPs, Annexin-V staining was performed. Annexin-V has great binding capacity for phosphatidylserine, which is externalized from the inner to the outer leaflet of the plasma membrane at early phase of apoptosis. This binding makes possible to measure the apoptosis by flow cytometric analysis. Using propidium iodide (PI) helps to distinguish apoptosis from necrosis due to difference in permeability of PI through the cell membranes of live and damaged cells.

The Annexin staining was carried out by Annexin-V FITC apoptosis detection kit to determine the percentage of apoptotic cells. Briefly, treated and untreated cells were harvested by centrifugation and washed twice in PBS. Propidium iodide staining was used as a control to differentiate cells undergoing necrosis. Paclitaxel (7.4 μM), an antitumor drug, was used as positive control [77]; nontreated cells were used as negative control. Cells ($1x10^6$) were seeded in six-well plate and allowed to attach for 24 h. After treating cells with 25.0 μg mL^{-1} NPs for 24 h, the detached and attached cells were collected and washed twice with ice-cold PBS. Subsequently, cells were resuspended in 500 μl of 1X binding buffer, 5 μl Annexin V-FITC and 10 μl of propidium iodide were added and incubated for 10 min at 37 °C in the dark. Thereafter, cells were analyzed using BectonDickinson FACSCalibur flow cytometry system. The number of viable, apoptotic and necrotic cells were quantified by flow cytometer and data analyzed by FACSComp software.

4.3.4. RNA Extraction and RT-PCR Analysis

The gene expression study was designed to investigate human dermal fibroblasts and A549 cells that express p53. Total RNAs were extracted for gene expression analysis using the high pure RNA isolation kit. The yield of RNA was determined by nanophotometer, and stored at −80 ^oC until use. For cDNA synthesis Senscript reverse transcriptase was used according to manufacturer's guide. In brief, 1000 ng of total RNA was mixed with 2 μl of 10X RT Buffer, 2 μl of deoxyNTPs mixture, 2 μl of 1 Mm Oligo dt primer, 1 μl of RNase inhibitor (10 unit), 1 μl of sencript reverse (50 U/μl) and incubated at 37 ^oC for 1 h

and placed on ice for 10 min and stored at −20 ^{o}C until use. Each sample for real-time RT-PCR analysis contained 200 ng of cDNA, SYBR Green Master Mix and 0.3 μM of each custom primer. The sense primer of p53 was 5'-CCTTCCCAGAAAACCTACCA-3' and the antisense primer was 5'-TCATAGGGCACCACCACACT-3'; these complementary sequences were located in exons 4 and 6, respectively, and the amplification product was a 371-bp fragment [78]. In the case of of β-actin, 5'-TCCTGTGGCATCCACGAAACT-3' was used as the sense primer, 5'-GGAGCAATGATCCTGATCTTC-3' was used as the antisense primer [14]. β-actin mRNA was employed as an internal standard, and each gene expression was determined by RT-PCR and normalized against β-actin mRNA levels. The PCR program cycles were set as 40 cycles of 94 °C for 30 s, 57 °C for 60 s, and 72 °C 60 s. The PCR amplification and real-time fluorescence detection were performed with a Bio-Rad iCycler Real-Time PCR system. PCR amplification was carried out according to the manufacturer's instruction (Applied Biosystems, CA). All PCR products were amplified in a linear cycle. Data are the mean ± SD from three samples per group of three independent experiments.

4.3.5. Western Blotting

To determine the presence of p53 protein, proteins were extracted from human dermal fibroblast and A549 cells at each time point during treatment with 25.0 μg mL^{-1} NPs. After the exposure, the cells were washed twice with ice-cold PBS and were lysed with RIPA lysis buffer (RIPA buffer, PMSF, sodium orthovanadate and protease inhibitor cocktail). Protein concentrations were determined using Bradford Assay. Protein lysates were supplemented with Laemmli buffer (125 Mm Tris-HCl, pH 6.8, 20% (v/v) glycerol, 4% (v/v) SDS, 10% (v/v) 2-β-mercaptoethanol and 0.004% bromphenol blue) and incubated for 5 min at 95 °C. Equal amounts of total cell protein (40 μg) were separated by SDS-PAGE (10%). The lysates were electrophoresed at 70V through the stacking gel (0.25 M Tris, 0.2% (w/v), SDS stock solution, pH 6.8) and at 90 V through the separating gel (0.75 M Tris, 0.2% (w/v), SDS stock solution (w/v), pH 8.8). After the SDS page, sheets of filter Whatman papers and membranes were pre-cut to the gel dimensions. PVDF membrane was activated by soaking in 100% methanol for 15 sec, washed with deionized water for 2 min and then equilibrated in cold transfer buffer (25 mM Tris, 200 mM glycine, 20% methanol, pH 8.5) for at least 5 min. The filter Whatman papers, sponges, membranes,

and gels were also immersed in cold transfer buffer for 5 min. The blotting sandwich assembled in the following order; anode of cassette, sponge, Whatman paper filter paper, PVDF membrane, Whatman paper filter paper, sponge, white part of cassette. For the greatest transfer efficiency, air bubbles should be completely removed from the sandwich by rolling a roller over the surface of each layer. Finally, power was applied and the electro-transfer was set up with constant current at 150 mA/cm^2 membrane area for 1.5 h. When the transfer was finished, the membrane was dissembled from the transfer stack and saturated in deionized water. After being electrotransferred were onto PVDF membranes, the membrane was blocked with 12.5 ml 1% blocking solution under constant shaking for 60 min. The p53 primary antibody (200 µg/ml, diluted 1:2500) was added 1% blocking solution and the membrane was incubated with primary antibody solution for overnight at +4 °C. The membrane was washed three times with TBS (0.1 M TrisHCl, 0.9% NaCl, 0.05% Tween-20, pH 7.4) for 15 min and then washed twice with 0.5% blocking solution for 20 min. The secondary antibody solution was used at 1:15000 for 2 h, and the membrane was washed three times with TBS. Antigen-antibody complexes were visualized by development with signal strength was detected by using the ECL advance western blotting detection kit as recommended. The protein bands were detected using the MFChemiBis 3.2 Bioimaging Systems. After imaging the p53 protein, the membrane was stripped (30 minutes at 50 °C) in stripping buffer containing 100 mmol/L 2-mercaptoethanol, 2% SDS, and 62.5 mmol/L Tris-HCl (pH 6.7). The stripped membrane was washed twice with TBS for 15 min. After washing the membrane, the membrane was blocked with blocking solution for 1 h at room temperature. The alfa-tubulin antibody solution (1:12500) was incubated with membrane for overnight at +4 °C. The procedure before visualization was the same with p53 antibody; alfa-Tubulin was used as an internal control. All Western blots were done at least thrice for each experiment.

4.3.6. Confocal Microscopy Imaging

The naked AgNPs, modified AgNPs and their aggregates within the cells were imaged using a Leica Confocal Microscopy. The cells were seeded on cover slips in a six-well plate at a density of 1×10^6 cells/well. After they were exposed to 25 µg/ml NPs, the medium was immediately added into the cell-NPs mixture and incubated for 24 h. The cover slips were washed three times with PBS and the cells were fixed with 2%

paraformaldehyde for 30 min at 4 °C. The fixed cells were washed three times, each for five minutes and the cells were viewed and imaged under a confocal laser scanning microscope. The images were processed using Leica Confocal software version (version 2.61). The surface plasmons of AgNPs aggregates in the cells were excited at 488 nm.

5. RESULTS AND DISCUSSION

5.1. CHARACTERIZATION OF NPS

The different size of NPs observed by TEM and SEM and an example from each type of NPs is shown in Figure 5.1. The synthesis of the AuNPs and AgNPs with different sizes and surface chemistry were confirmed with UV-Visible spectroscopy and their absorption spectra are presented in Figure 5.2. The absorption peaks of NPs are in good agreement with the literature values.

The synthesized AuNPs had a maximum absorbance at 520 and 530 which is a characteristic surface plasmon resonance band for 13 nm and 50 nm AuNPs, respectively. Figure 5.1 (a) shows the transmission electron microscopy TEM image of 13 nm AuNPs synthesized as described here.

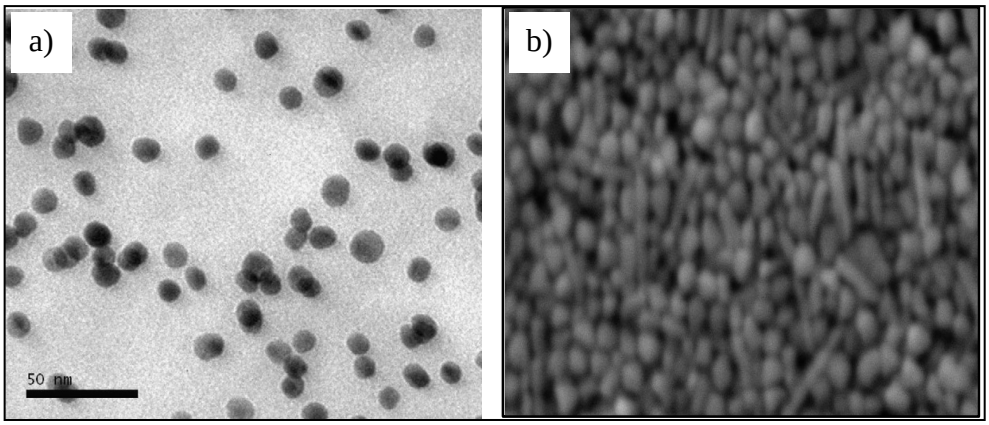

Figure 5.1. The TEM images of 13 nm AuNPs (a) and SEM image of 50 nm AgNPs (b)

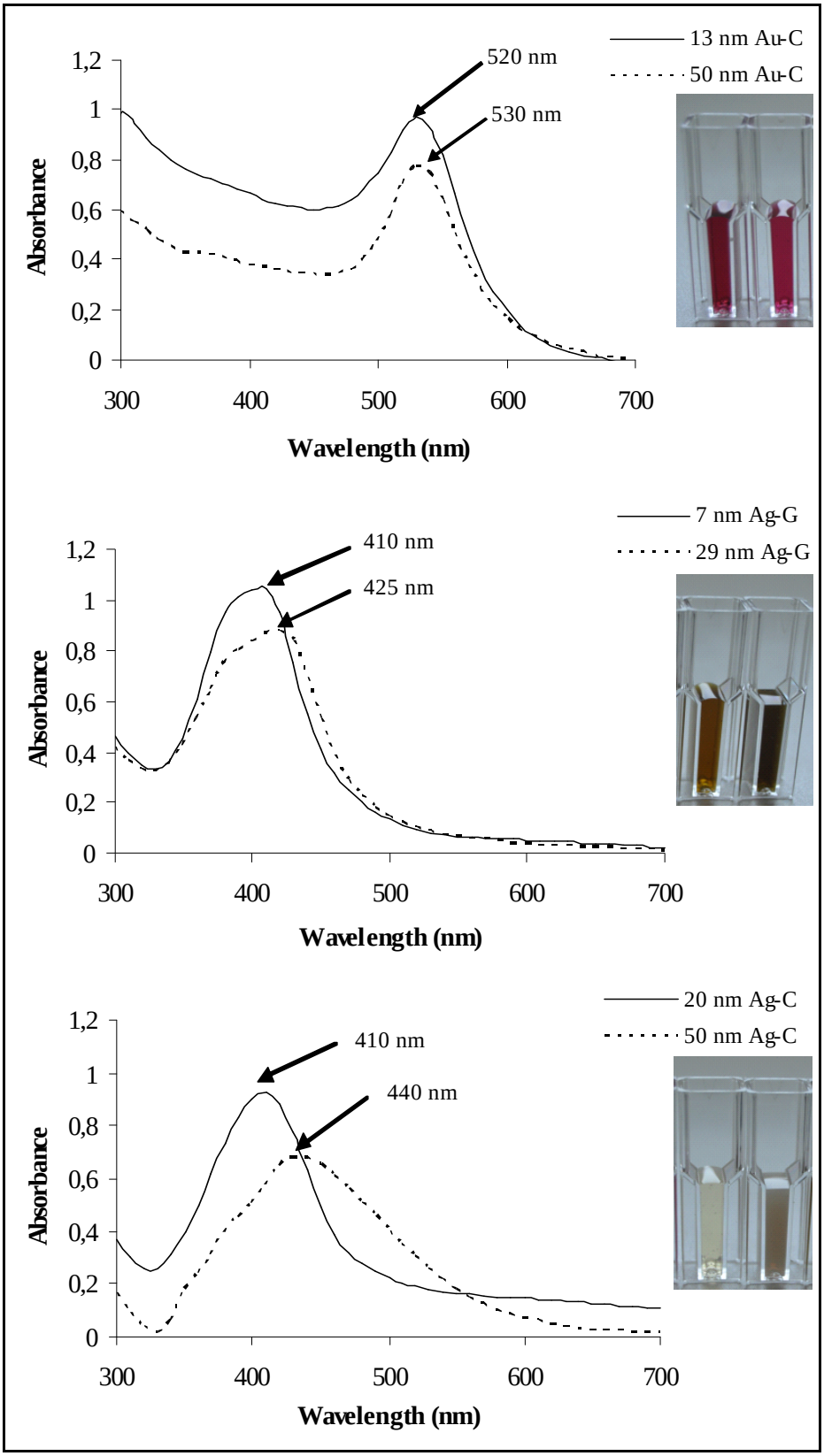

Figure 5.2. The UV–Vis absorption spectra of AuNPs and AgNPs of different sizes

All AgNPs containing suspensions show characteristic surface plasmon band on UV/VIS spectrum. A 7 nm AgNPs containing suspension has a narrow band at a maximum of 410 nm while a 29 nm AgNP suspension shows the maximum at 425 nm. The red shift on the maximum is due to the increased particle size. It is known that prepared AgNPs with Lee method have 420 nm absorption peaks and the size of NPs is in the range of 40-60 nm. Figure 5.2 shows the AgNPs absorption maximum at 410 nm and 440 nm for 20 nm and 50 nm AgNPs. The 50 nm AgNPs synthesized with Lee method observed by SEM are shown in Figure 5.1 (b).

Although TEM and SEM contributes the visualization of 13 nm AuNPs and 50 nm AgNPs, it is does not provide the real size distribution and behavior of the NPs in suspension. Dynamic light scattering (DLS) is a non-invasive method to measure the size of NPs in a colloidal suspension.

Table 5.1. The hydrodynamic diameter of NPs

NPs	Hydrodynamic diameter (nm)						
	In water	In Media					
		F-12 HAM			DMEM		
		1 day	2 day	3 day	1 day	2 day	3 day
13 nm Au-C	28 ± 3	31 ± 3	46 ± 2	47 ± 1	91 ± 1	107 ± 3	112 ± 1
50 nm Au-C	53 ± 1	76 ± 2	89 ± 4	124 ± 3	117 ± 3	136 ± 3	138 ± 3
7 nm Ag-G	14 ± 2	33 ± 1	35 ± 2	36 ± 2	70 ± 1	83 ± 2	88 ± 2
29 nm Ag-G	42 ± 2	49 ± 4	50 ± 2	57 ± 2	43 ± 1	47 ± 3	66 ± 1
20 nm Ag-C	38 ± 2	120 ± 2	133 ± 1	138 ± 2	120 ± 1	129 ± 2	134 ± 5
50 nm Ag-C	79 ± 1	111 ± 1	114 ± 3	114 ± 1	110 ± 1	127 ± 3	132 ± 3
Ag / Lactose	88 ± 1	123 ± 1	130 ± 2	130 ± 1	195 ± 1	213 ± 2	218 ± 2
Ag / ssDNA	94 ±1	132 ± 3	144 ± 2	146 ± 1	210 ± 1	225 ± 2	230 ± 2

We also investigated the physical properties of the NPs before and after exposure to the cell culture conditions. Therefore, it is demonstrated that the AuNPs are taken into the cell upon nonspecific binding of serum proteins on the surface of AuNPs, which in turn

mediates uptake of NPs [14]. The surface characteristics of NPs effect their internalization into living cells. The DLS results for particle size in their suspension and culture media for the AuNPs and AgNPs are presented in Table 5.1. All the size of NPs tended to increase when dispersed in water and cell culture media. The 13 nm and 50 nm AuNPs ranged from 28 and 53 nm in water to 31 and 76 nm in F-12 HAM media, 91 and 117 nm in DMEM (high glucose) media, respectively. The 7 nm and 29 nm AgNPs were 14 nm and 42 nm in water, 33 nm and 49 nm in F-12 media, and 70 nm and 43 nm in DMEM media, respectively. The 20 nm and 50 nm AgNPs showed a change in size when compared dispersion in water to F-12 media, from 38 to 120 nm and 79 to 111 nm, respectively. The 20 nm and 50 nm AgNPs also formed increased size of particles in DMEM media with values of 120 and 110 nm, respectively. Their sizes in water were 88 and 94 nm, while in F-12 HAM media, sizes were 123 and 132 nm for lactose and oligonucleotide modified AgNPs, respectively. As seen in Table 5.1, the NPs revealed a similar pattern by increasing the size when dispersed in either F-12 HAM or DMEM. However, the 13 nm and 50 nm AuNPs was an exception to this trend showing an increase from 31 nm and 76 nm in F-12 HAM to 91 nm and 117 nm in DMEM media with high glucose, respectively.

As seen, NPs were mixed with the cell culture media; the size distributions of NPs were significantly influenced. The hydrodynamic diameters of all NPs were increased due to the adsorption of serum proteins onto the NPs. The size increment for all the NPs was in the range of 26–37 nm when they are added into the media. The increase of the size of NPs can be understood by considering the sizes of proteins, which are in the range 5–6 nm (60 kDa), two or three layers of proteins on the NPs. The NPs in media showed approximately a 10% increase in size when incubated for 2 day and 3 day compared to 1 day. For instance, the 50 nm AuNPs in F-12 HAM media showed an increasing trend from 76 nm for 1 day incubation to 89 nm for 2 day incubation and finally 124 nm for 3 day incubation. From the size distribution, it is evident that there is almost no aggregation in the media.

Table 5.2. The zeta potentials of NPs

NPs	Zeta potential (mV)						
	Dispersed in water	In Media					
		F-12 HAM			DMEM		
		1 day	2 day	3 day	1 day	2 day	3 day
13 nm Au-C	-30 ± 2	-4 ± 1	-3 ± 1	-3 ± 1	-11 ± 1	-10 ± 3	-9 ± 1
50 nm Au-C	-51 ± 1	-6 ± 1	-5 ± 1	-4 ± 1	-10 ± 1	-8 ± 1	-5 ± 3
7 nm Ag-G	-19 ± 3	-8 ± 1	-10 ± 1	-8 ± 1	-7 ± 1	-9 ± 2	-9 ± 2
29 nm Ag-G	-36 ± 1	-9 ± 1	-8 ± 1	-9 ± 1	-10 ± 1	-11 ± 1	-11 ± 1
20 nm Ag-C	-45 ± 1	-10 ± 2	-10 ± 1	-5 ± 2	-9 ± 1	-7 ± 2	-6 ± 5
50 nm Ag-C	-35 ± 1	-9 ± 1	-7 ± 1	-5 ± 1	-10 ± 1	-12 ± 2	-9 ± 2
Ag / Lactose	-31 ± 1	-9 ± 1	-9 ± 1	-9 ± 2	-9 ± 1	-11 ± 1	-8 ± 1
Ag / ssDNA	-30 ±1	-9 ± 1	-9 ± 1	-10 ± 1	-11 ± 1	-13 ± 1	-9 ± 1

The accumulation of proteins can influence the charge density on NPs. Therefore, the surface charge potential of NPs was also evaluated. The results from reading the zeta potential of NPs are also shown in Table 5.2. The 7 nm AgNPs have the highest zeta potential with -19 mV while most particles had zeta potentials around -30–35 mV, 50 nm AuNPs possesses the lowest at -51 mV. However, as the NPs are mixed with the media, the surface charge of NPs decreases due to the adsorption of the serum protein onto the NPs as seen Table 5.2.

Based on the DLS data, it is clear that addition of NPs into culture media significantly alter the surface properties of NPs that result with the increased size of NPs. The surface properties and size of NPs eventually define their interactions with living cells.

5.2. CYTOTOXICITY OF NANOPARTICLES

The human dermal fibroblast and A549 cells treated with NPs at 12.5, 25.0, 50.0 and 100.0 μg ml^{-1} concentration levels for the incubation of three days were subjected to MTS assay for cell viability determination. Figure 5.3 and 5.4 show the cell viability of the NPs

for two living cells; healthy human dermal fibroblast and cancerous A549 cells. There was no pronounced effect on cell viability for all NPs at the concentration of 12.5 μg ml^{-1} except small decreases with the use of 7 nm AgNPs and 29 nm AgNPs at 72 h. The cell viability treatment by NPs at a concentration of 100.0 μg ml^{-1} decreased dramatically in both AuNPs and AgNPs. The cell viability of small size NPs treated human dermal fibroblast and A549 cells was higher than that of the large NPs treated cell lines, and AgNPs had more negative effect on cell viability than AuNPs of the same size.

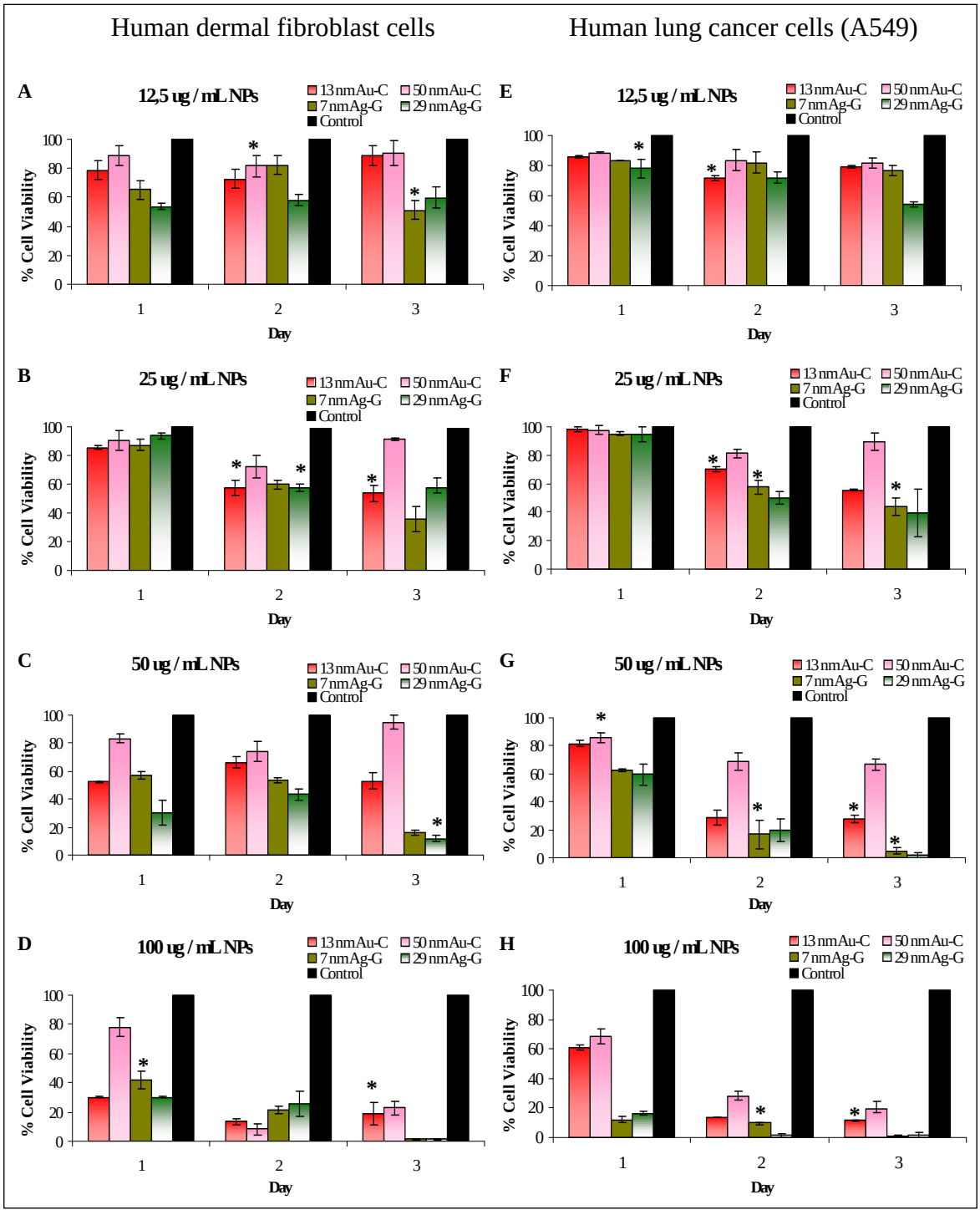

Figure 5.3. Evaluation of the cytotoxicity of NPs. Percent viability of human dermal fibroblast A–D and A549 cells E–H during three-day incubation period in the presence of 12.5, 25.0, 50.0 and 100.0 μg ml^{-1} NP concentrations. The values represent the mean of three separate experiments; * denotes $P < 0.05$ as obtained using Student's t -test, where the statistical significance between untreated and NP-treated samples was analyzed for each concentration

The effect of AuNPs and AgNPs on cell viability of human dermal fibroblast cells is presented in Figure 5.3 and 5.4. At the 12.5 μg ml^{-1} concentration level, 50 nm AuNPs cause approximately 10% loss in viability in the human dermal fibroblast cells while 7 nm AgNPs, synthesized with gallic acid, show 51% cell viability for three days. When the impact of NPs size was compared, the small NPs had more negative effect on the cell viability than large NPs for human dermal fibroblast cells. The inspection of the figures reveals that the modifying AgNPs with lactose or oligonucleotide changes the cell viability in a positive way as seen in Figure 5.4. For the human dermal fibroblast cells, the cytotoxicity was evident even after 1 day exposure to 100.0 μg $ml^{-1}$of NPs.

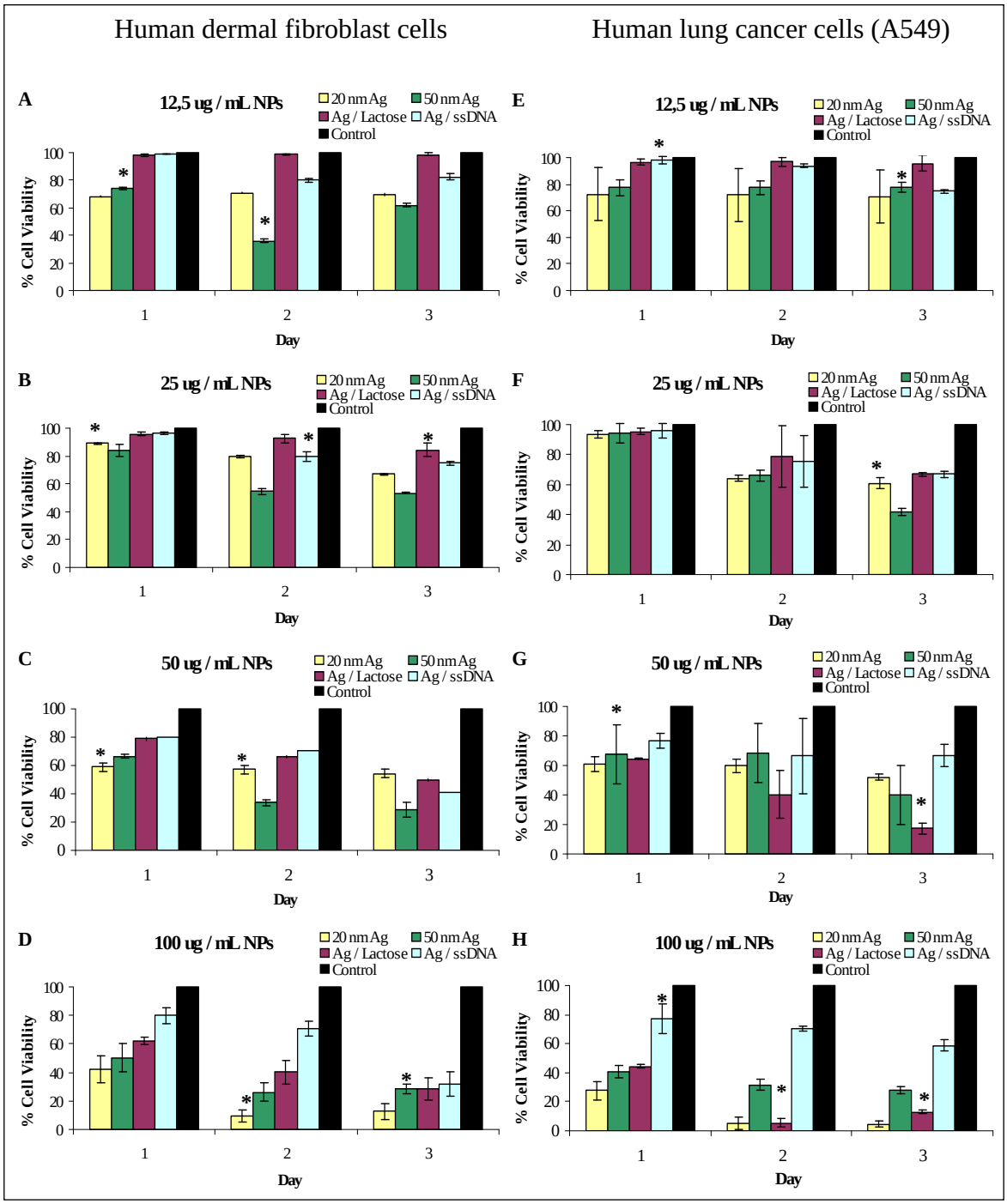

Figure 5.4. Evaluation of the cytotoxicity of NPs. Percent viability of human dermal fibroblast A–D and A549 cells E–H during three-day incubation period in the presence of 12.5, 25.0, 50.0 and 100.0 μg ml^{-1} nonmodified and modified AgNP concentrations. The values represent the mean of three separate experiments; * denotes $P < 0.05$ as obtained using Student's t -test, where the statistical significance between untreated and NP-treated samples was analyzed for each concentration

Figure 5.3 and 5.4 show the toxic effect of the NPs on A549 cancerous cells. As seen, NPs show toxic effect on cancer cells as the concentration and incubation time are increased. When compared to the toxicity of 29 nm AgNPs to healthy human dermal fibroblast cells (11.88%), it is apparent that 29 nm AgNPs show a higher toxicity on the A549 cells (1.42%). This toxic effect becomes much more significant at 50.0 μg ml^{-1} concentration level. Specifically, the results suggest that in the presence of the oligonucleotide modified AgNPs there is a higher percentage of cell viability (58.65%) with either longer exposure or higher concentrations in comparison to that with the 50.0 nm AgNPs (27.93%). The results of MTS assay for A549 cells showed a similar concentration and time dependent response with a loss in cell viability at 50.0–100.0 μg ml^{-1} on 2 day and 3 day treatment.

5.3. GENOTOXICITY OF NANOPARTICLES

To our knowledge, this is the first report documenting the effect of different size and surface chemistry of NPs on DNA damage. The DNA damage effect of the synthesized NPs on cells was investigated at 12.5, 25.0, 50.0 and 100.0 μg ml^{-1} concentration levels for the duration of three days. Figure 5.5 shows the fluoresence microscopy images of the genotoxicity of the NPs for two model cells: healthy human dermal fibroblast and cancerous A549 cells. The alkaline single-cell gel electrophoresis results showed a dose-time dependent increase of tail momentum for human dermal fibroblast and A549 cells.

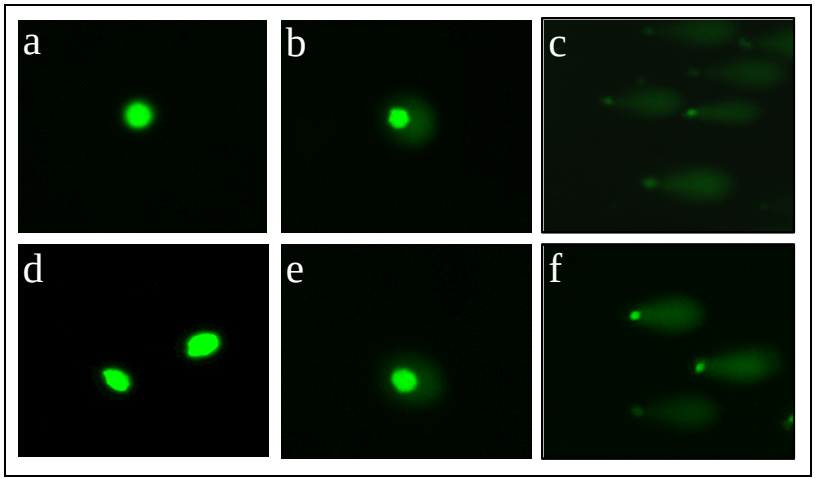

Figure 5.5. Comet analysis: untreated (a), 13 nm AuNPs treated (b), and 29 nm Ag-NPs treated (c) human dermal fibroblast cells; untreated (d), 13 nm AuNPs treated (e), and 29 nm Ag-NPs treated (e) A549 cells stained by SYBR green (concentration of NPs 25.0 µg mL^{-1})

For human dermal fibroblast cells, the influence of synthesized NPs on cellular DNA damage is seen in Figure 5.6 and 5.7. At 12.5 and 25.0 µg ml^{-1} concentrations, the AuNPs didn't cause noteworthy tail momentum for the human dermal fibroblast cells during the three days as seen in Figure 5.6. Analysis of tail momentum values did not show DNA damage induction after 3 day of exposure to 12.5-25.0 µg ml^{-1} 50 nm AuNPs. While in human dermal fibroblast cells exposed for 1 day to 50 nm AuNPs tail momentum was found at 1.44 µm, exposed to 7 nm AgNPs a significant induction of DNA damage was found at 5.37 µm. For all concentrations of 7 nm and 29 nm AgNPs exhibited higher DNA damage than other NPs and at 100.0 µg ml^{-1} concentration, and the DNA damage significantly increased for the last two days. With the increasing concentration of NPs, a shift from a low DNA damage category (tail momentum< 2), in control, to high DNA damage category (tail momentum> 4) in treated human dermal fibroblast cells, was observed in Figure 5.6 and Figure 5.7.

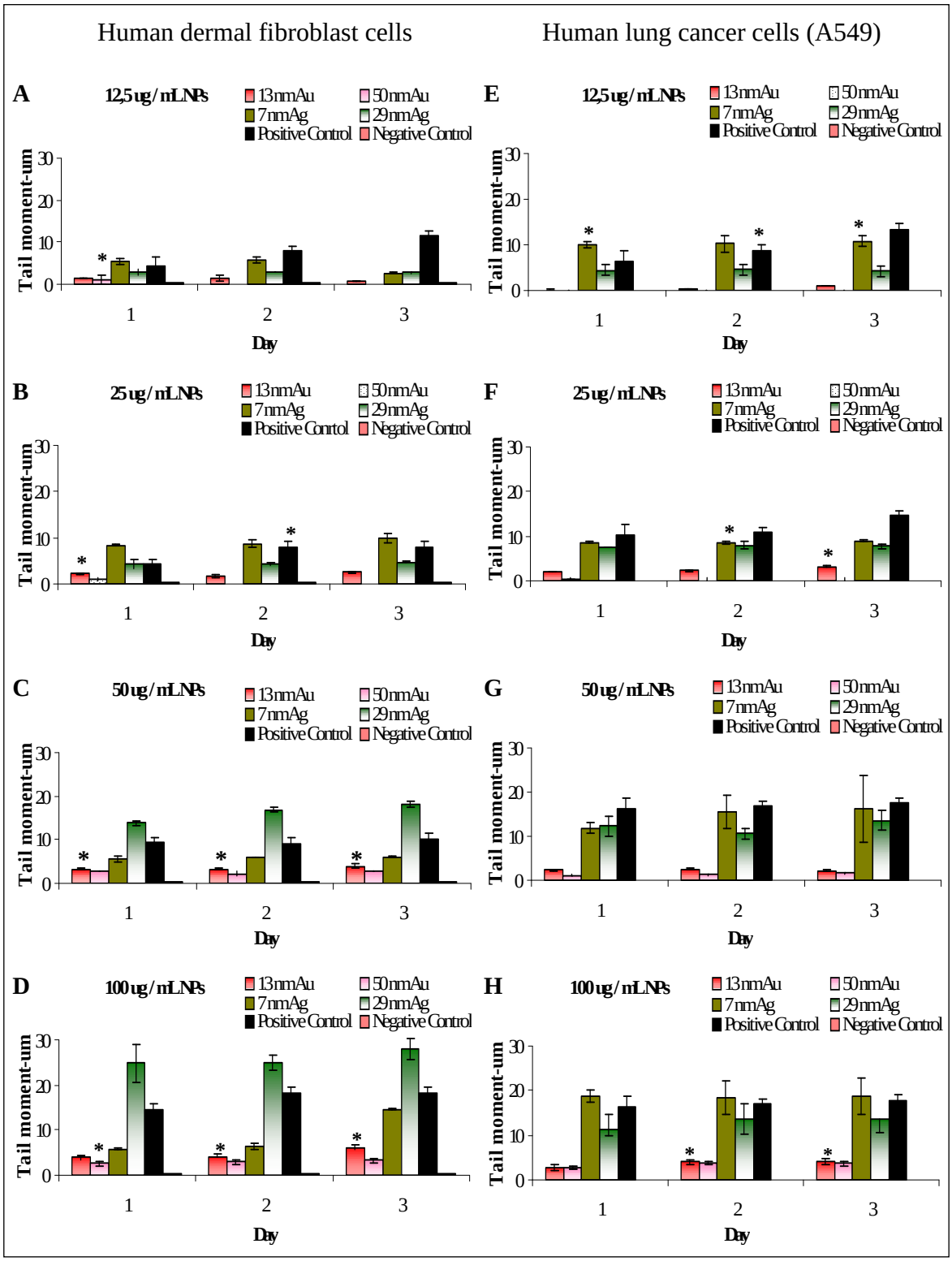

Figure 5.6. Comet analysis: untreated and NPs treated human dermal fibroblast cells (A-D) and untreated and NPs treated A549 cells (E-H) stained by SYBR green. *represents $P<0.05$

By considering the result represented in Figure 5.7, a significant induction in DNA damage was observed in human dermal fibroblast cells exposed to AgNPs for 24 h at 50.0 and 100.0 μg ml^{-1} concentrations compared to control as evident by Comet assay parameters tail momentum. Corresponding to the treatment with the highest dose, this is only oligonucleotide modified AgNPs well below the concentrations tested and found to have slight effect on tail momentum in human dermal fibroblast cells (100.0 μg ml^{-1}). Although 20 nm AgNPs show more genotoxicity than 50 nm AgNPs during three days, modifying 50 nm AgNPs with lactose and oligonucleotide change appreciably for all concentrations Figure 5.7 A-D.

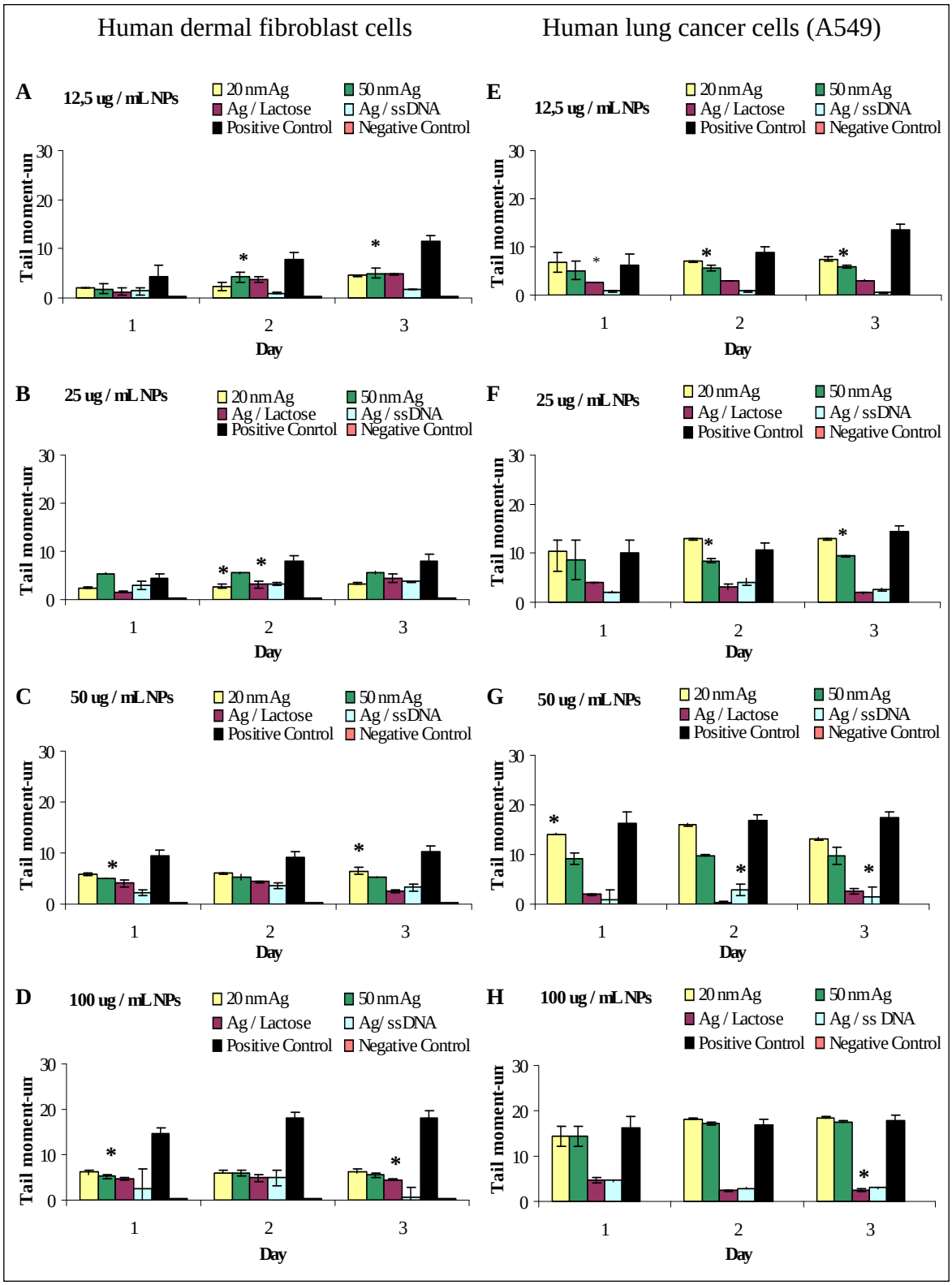

Figure 5.7. Comet analysis: untreated and nonmodifed or modified AgNPs treated human dermal fibroblast cells (A-D) and untreated and nonmodifed or modified AgNPs treated A549 cells (E-H) stained by SYBR green. *represents $P<0.05$

The NPs caused statistically significant concentration depend DNA damage in A549 cells as measured by the comet assay parameters. As seen in Figure 5.6 (E-H), 13 nm and 50 nm AuNPs have no significant cellular DNA damage at 12.5-25.0-50.0 µg ml^{-1} concentrations and the cellular DNA damage becomes more apparent with increasing concentration to 100.0 µg ml^{-1}. In Figure 5.6 (E-H), the 7 nm and 29 nm AgNPs behave more genotoxic during three days at 12.5 and 25.0 µg ml^{-1} concentrations while 13 nm and 50 nm AuNPs show genotoxicity to a lesser extent. However, the genotoxic effect of both types of AgNPs increases significantly with the three-day incubation. Increasing the concentration to 100.0 µg ml^{-1} significantly influences the cellular DNA damage for all types of NPs. At 100.0 µg ml^{-1} concentration level, the highest DNA damage was detected for 7 nm AgNPs as seen Figure 5.6 H. At the same concentration, the 7 nm AgNPs was most potent (18.85 µm tail momentum) and the other NPs; 20 nm AgNPs (18.53 µm tail momentum), 50 nm AgNPs (17.6 µm tail momentum) and 29 nm AgNPs (13.78 µm tail momentum) caused pronounced increase of DNA damage for A549 cells during 3 day treatment. Interestingly, the exposure of modified AgNPs consistently showed elevated levels of DNA damage for different concentrations of AgNPs either lactose modified AgNPs or oligonucleotide modifed AgNPs.

Compared to gallic acid sythesized AgNPs, sodium citrate synthesized AgNPs resulted in a lower genotoxicity response at the same concentration levels. This change can be attributed to the fact that the AgNPs have different surface chemistry.

5.4. EFFECT OF NPs ON CELL APOPTOSIS AND NECROSIS

In order to investigate the basis of cell death induced by NPs, we performed apoptosis analysis using the flow cytometry. Since the cellular metabolic activity seemed affected by the NPs, we assessed the possibility (A lower concentration of NPs was chosen as a more realistic scenario) of apoptosis caused by the NPs, especially at low concentration (25.0 µg ml^{-1}). Using the apoptosis assay that measures the number of cells in apoptosis versus necrosis, we confirmed that apoptosis took place at low NPs concentration. The apoptosis assay findings are demonstrated that the cell death arise from apoptosis and necrosis of cells following the NPs treatment.

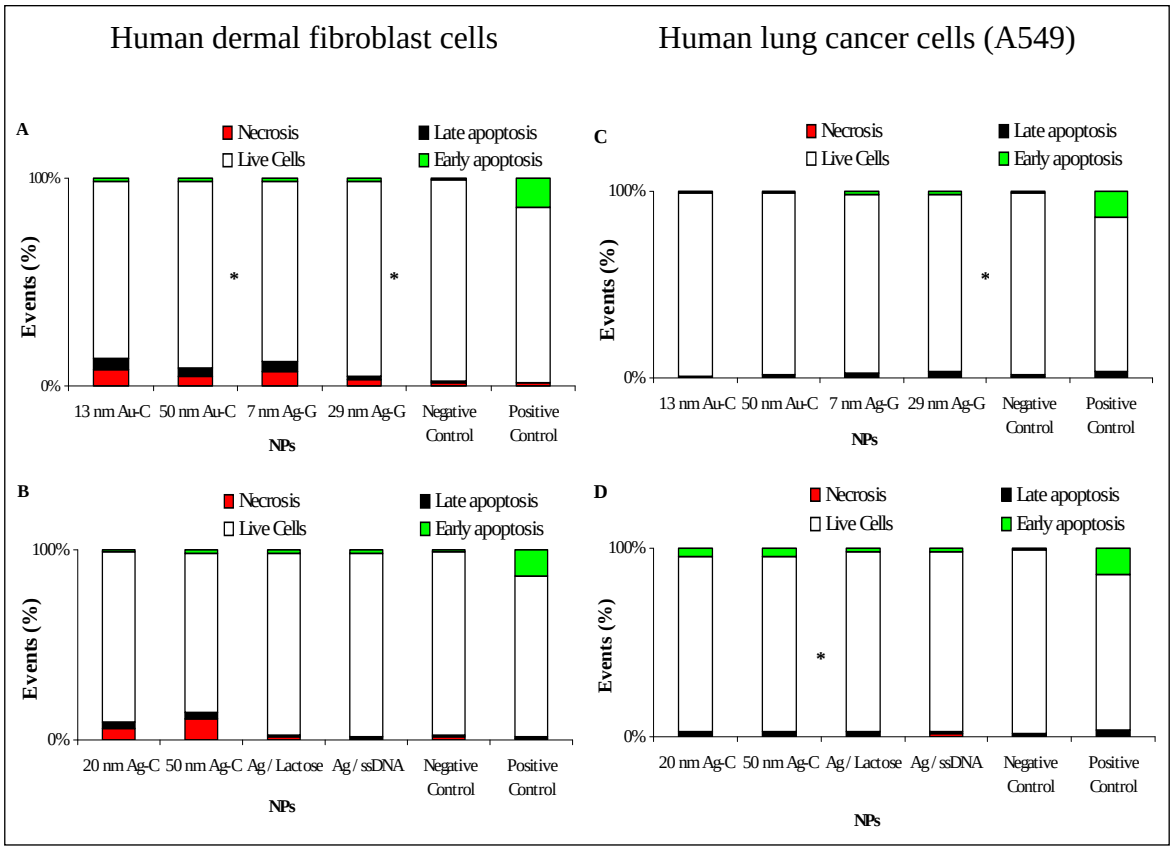

Figure 5.8. Annexin-V staining of human dermal fibroblast and A549 cells to detect apoptosis and necrosis. The viable cell percentage is greater than the death cells. Only FITC stained cells are signified as early apoptotic, whereas only PI stained cells are signified as necrotic. At the late apoptosis the cells internalize both stains. * represents $P < 0.05$

In order to examine whether treatment with NPs leads to adverse effects for the human dermal fibroblast cells, we investigated the rate of early, late apoptosis and necrosis. Figure 5.8 shows the percentage of cells undergoing apoptosis exposed to different NPs concentrations and incubated for 24 h. As shown in Figure 5.8, NPs induced apoptosis in a surface chemistry dependent manner. Although the ratio of early apoptosis to total apoptosis was frequent at 25.0 μg ml^{-1} AgNPs (synthesized with sodium citrate), the late-apoptosis ratio became remarkable for 13 nm, 50 nm AuNPs and 7 nm AgNPs. The apoptosis induction by 13 nm AuNPs (6.2%) was stronger than by other NPs in agreement with the result of cytotoxicity, Figure 5.3. These results indicated that apoptosis took part in

the mechanism of cell death by NPs. More cells became necrotic as the human dermal fibroblast cells were exposed to 50 nm AgNPs (11.36%).

Figure 5.8 C-D illustrates apoptosis in the A549 cells treated with NPs concentration of 25.0 µg ml^{-1}. In the case of treatment with AgNPs, apoptotic cells began to be observed and few necrotic cells were observed in oligonucleotide modified AgNPs. However, A549 cells exhibited lower necrotic cells compared to human dermal fibroblast cells. Apoptosis results with A549 cells indicated that the positive control (paclitaxel) had an apoptosis level of approximately 18%. Apoptosis measurement for 20 nm (6.54%), 29 nm (5.16%), 50 nm (6.67%) AgNPs and lactose modified AgNPs (4.25%) treatment was significantly different when compared to the negative control (2.28%). This suggests that at 25.0 µg ml^{-1} concentration, these NPs are able to cause significant apoptosis effect on A549 cells. On the other hand, when apoptosis was measured 24 h after exposed to 13 nm (0.84%-087%) and 50 nm (0.67%-1.59%) AuNPs and oligonucleotide modified AgNPs (1.63%-1.17), early and late apoptotic cells were low. The results demonstrated an apoptotic effect on A549 cells when they were exposed to 50 nm AgNPs.

5.5. EFFECT OF NANOPARTICLES ON p53 GENE EXPRESSION

To answer the question how the p53 gene expression in human dermal fibroblast and A549 cells is changed after NP treatment. Treatment of human dermal fibroblasts and A549 cells with NPs resulted in DNA damage and increased expression of p53 gene and apoptosis. Figures 5.9 A-B presents the gene expression of human cells treated with the NPs for 6 and 24 h.

For the human dermal fibroblast cells, it was evident that p53 gene were up-regulated after treatment with 20 nm AgNPs (0.83) at 25.0 µg mL^{-1} for 6 h. At the same time, the expressions of p53 gene in the modified AgNPs were relatively lower. In the lactose or oligonucleotide modified AgNPs, the lower percentage of DNA damage and apoptosis in human dermal fibroblast cells paralleled with the lower level of p53 gene expression in these cells at 6 h. The results have been confirmed that p53 gene appears to be a fundamental factor in the apoptotic pathway triggered by DNA damaging agents. After the

long-term incubation, the expression levels of p53 gene downregulated compared to those at short term.

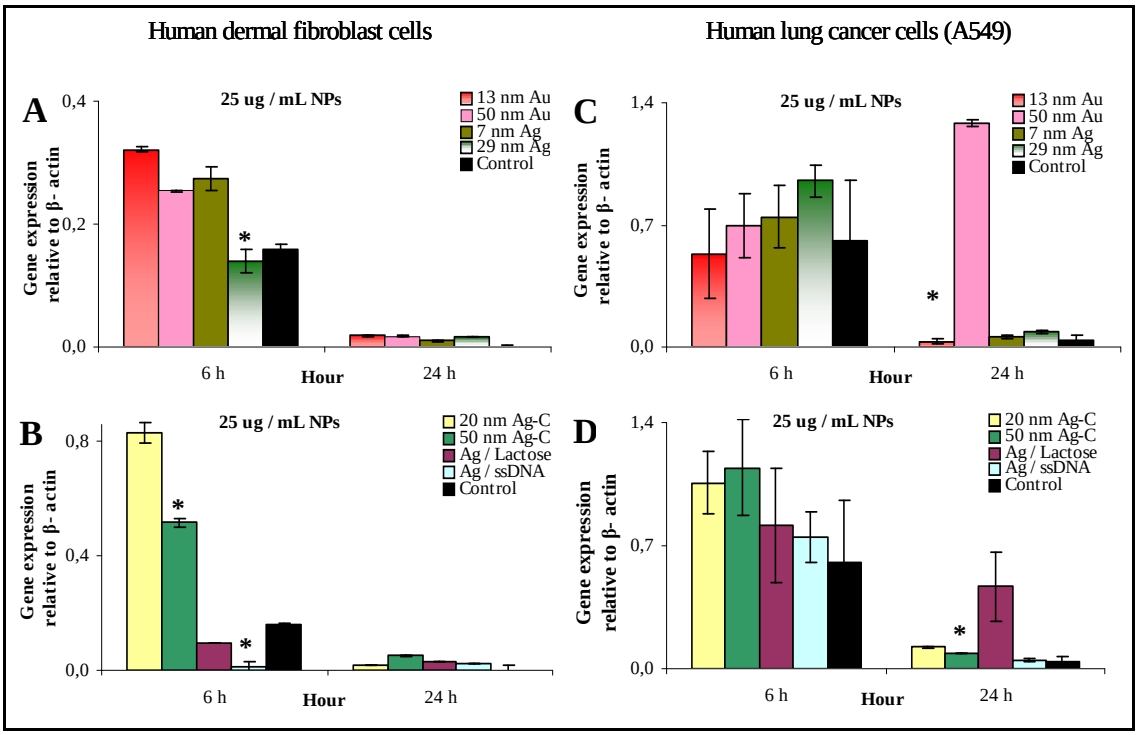

Figure 5.9. Gene expression of p53 in human dermal fibroblast and A549 cells incubated with culture medium containing NPs at 25.0 µg mL^{-1} for 6 and 24 h by RT-PCR. Significance $p<0.05$: * higher than control

In A549 cells at 6 h, the expressions of p53 gene in AgNPs-treated cells were higher than those in AuNPs-treated groups for any size of the NPs. These findings are in good agreement with DNA damage and apoptosis levels, AgNPs induced DNA damage and apoptosis were higher than AuNPs for A549 cells as seen in Figure 5.6, 5.7, 5.8, 5.9. In A549 cells, p53 gene expression and the percentage of apoptosis was the highest when treated with 50 nm AgNPs (1.15) treated cells at 6 h. This supports the idea that the NPs exposed to A549 cells upregulated the p53 gene in order to provide a rapid response to DNA damage before proceeding to apoptosis. Furthermore, the lactose modified AgNPs caused significant p53 expression and apoptosis in A549 cells, while the degree of these mechanisms is low in the human dermal fibroblast cells.

The expressions of p53 gene decreased at 24 h while there was a significant increase in p53 gene expression for the 50 nm AuNPs (1.29) treatment. With the treatment of lactose modified AgNPs cells, p53 gene expression decreased at 24 h. After treatment with lactose modified AgNPs (0.47), upregulation of the p53 gene would be active in evaluating and repairing DNA or, failing, in induction of apoptosis in A549 cells with severely damaged DNA. This condition would explain the p53-mediated response leading to the rapid apoptosis of A549 cells that we have observed with apoptosis assay.

5.6. EFFECT OF NANOPARTICLES ON p53 PROTEIN EXPRESSION

To assess the effects of the NPs in living cells, western blotting was performed to understand the levels of p53 protein expression. The presence of p53 protein was determined 6 and 24 h after exposure to NPs as seen in Figure 5.10. The western blot results demonstrated the presence of p53 protein after treatment with NPs in the human dermal fibroblast and A549 cells.

Figure 5.10 clearly demonstrates that treatment of the human dermal fibroblast cells with NPs, led to an up-regulation of the cell-cycle inhibitor protein p53 in a time-dependent manner. The p53 protein expression began to decrease in human dermal fibroblast cells after 6h. Additionally, these results suggest that different cell types respond differently to the NP treatment.

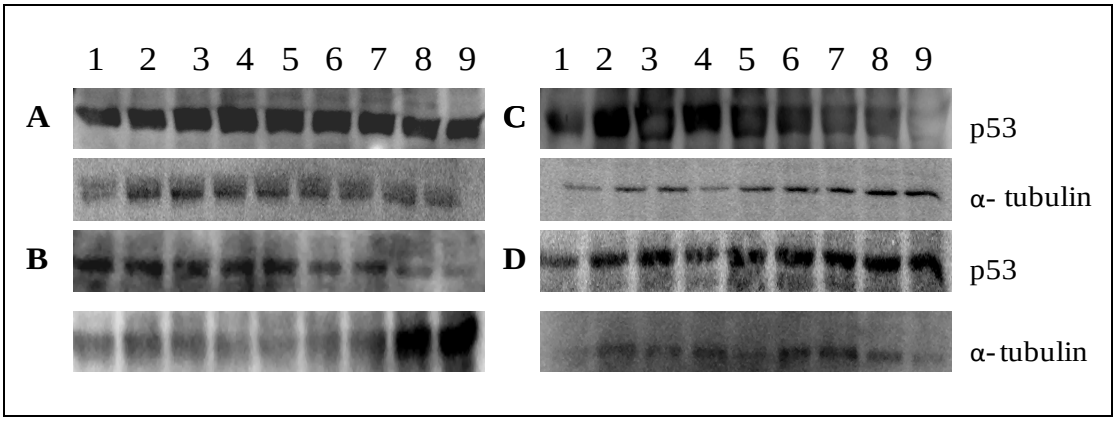

Figure 5.10. NPs up-regulated and activated the p53 protein in mammalian cells. The treated and untreated cells were lysed with RIPA buffer, and cell extracts subjected to western blots with p53 monoclonal antibody. A) Human dermal fibroblast cells The lanes 1–5 are as follows: lane 1 13 nm AuNPs treatment; lane 2 50 nm AuNPs treatment; lane 3 20 nm AgNPs treatment; lane 4 50 nm AgNPs treatment; lane 5 7 nm AgNPs treatment; lane 6 29 nm AgNPs treatment; lane 7 lactose modified AgNPs treatment; lane 8 oligonucleotide modified AgNPs treatment; lane 9 untreated cells after 6 h. The alfa tubulin blot as loading control. (B) The human dermal fibroblast cells after 24 h treatment. The order is the same as panel A. (C) Western blot of treated and untreated A549 cells after 6 h. The order is the same as panel A. (D) Western blot of treated and untreated A549 cells after 24h. The order is the same as panel A

A549 cells showed an additional upper band in response to treatment with NPs. From the p53 gene expression and western blot data, we conclude that significant induction of p53 protein expression after treatment with 50 nm AgNPs causes apoptosis in A549 cells. Annexin V staining further confirmed apoptotic death in the A549 cells with the extent of apoptosis correlating with p53 gene and protein levels. These results indicate that apoptosis in the human dermal fibroblast and A549 cells in response to NPs is mainly p53-dependent.

5.7. CELLULAR LOCALIZATION OF NANOPARTICLES

The cellular lozalization of NPs was monitored using confocal microscopy at the end of the first day at 25.0 µg ml^{-1} concentration level. The aggregates of AgNPs were visualized by exciting the surface plasmons of AgNP aggregates. Figure 5.11 shows the

aggregates of AgNPs and lactose, oligonucleotide modified AgNPs in both human dermal fibroblast and A549 cells. The inspection of the images show that the AgNPs aggregated in the cytoplasm and the lactose modified AgNPs formed larger aggregates in A549 cells than in human dermal fibroblast cells as seen in figure 5.11 (g).

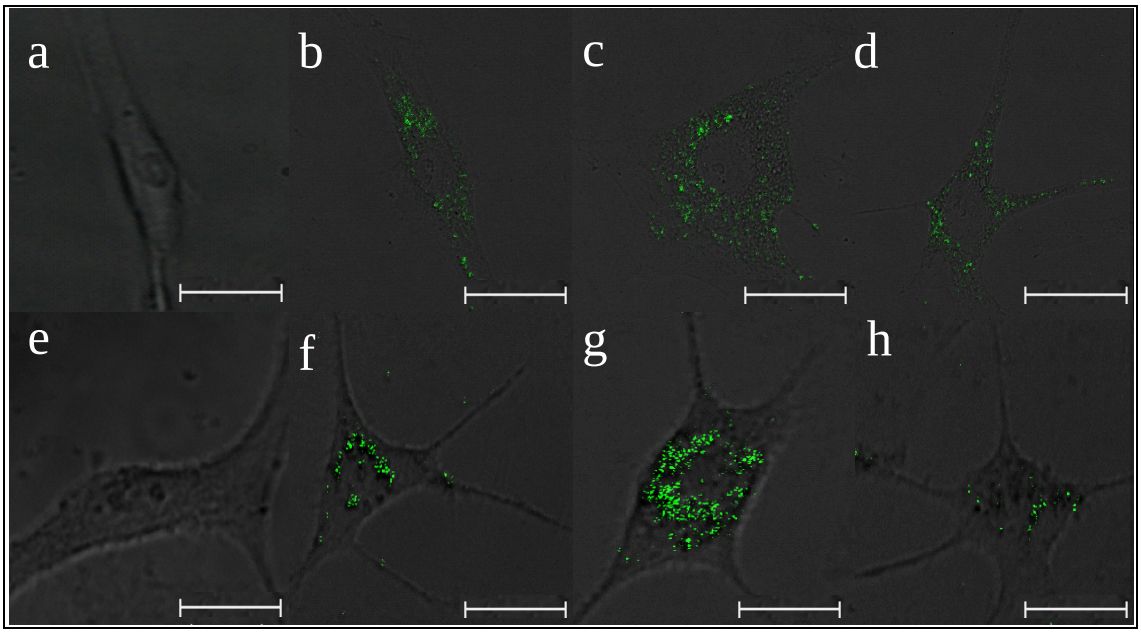

Figure 5.11. Confocal microscopy images of human dermal fibroblast (a) and A549 cells (e) without any treatment. The images of human dermal fibroblast (b) and A549 cells (f) after treatment with naked AgNPs. The human dermal fibroblast and A549 cells treated with lactose modified AgNPs (c-g), oligonucleotide modified AgNPs (d-h), respectively. (Bar scales are 10 µm for all images)

6. CONCLUSION AND RECOMMENDATIONS

6.1. CONCLUSION

For the application of NPs in nanomedicine, it is important to understand the cellular mechanism that NPs caused. The purpose of this thesis was to elucidate the NP induced cytotoxicity, cellular DNA damage, apoptosis and p53 gene expression in order to provide valuable information at molecular level effects of NPs.

The results suggest that all NPs reveal significant different effects on cell mechanism, which depends on their surface chemistry and size differences. As it could be concluded from the cytotoxicity and cellular DNA damage studies, AuNPs and AgNPs caused different levels of DNA damage in two types of human cells, especially 7 nm and 29 nm AgNPs exhibited more severe damage than other NPs. In agreement with the findings of others, [14,56] we have presented here some evidence that the small size NPs caused more cytotoxicity. For the cancer cells, the highest apoptosis and p53 gene expression (at 6 h) observed in 50 nm AgNPs should be model NPs for treatment of cancer cells using direct injection to tumor.

As a conclusion, this thesis demonstrates that lactose modified AgNPs in cancer cells cause DNA damage, lead to increase p53 expression, thereby resulting in apoptosis and in healthy cells doesn’t cause necrosis. In this extent, lactose modified AgNPs have paramount effects on function of cancer cells. These findings may suggest a novel method by which lactose modified AgNPs can be used as a unique anticancer therapeutic material. It bridges the field of nanoscience and medicine with the therapy in cancer cells and opens up the opportunity of utilizing the technological advances of nanoscience in the treatment of cancer.

6.2. RECOMMENDATIONS

This *in vitro* study of high level elicitation of viability, DNA damage, apoptosis and p53 gene expression of NPs treated cells will need to be further investigated to determine *in vivo* results. Even though the exact mechanism of this unique role of NPs is a subject of future investigation, the fact that NPs are endowed with such a function is extremely significant in the therapeutic application of NPs in medicine.

REFERENCES

1. Bianco, A., R. Sainz, S. Li, H. Dumortier, L. Lacerda, K. Kostarelos, S. Giordani, and M. Prato, "Biomedical applications of functionalised carbon nanotubes", Medicinal Chemistry and Pharmacological Potential of Fullerenes and Carbon Nanotubes, pp. 23–50, 2008.

2. Smith, J. E., L. Wang, and W. Tan, "Bioconjugated silica-coated nanoparticles for bioseparation and bioanalysis", TrAC Trends in Analytical Chemistry, Vol. 25, No. 9, pp. 848–855, 2006.

3. Wild, M., S. Berner, H. Suzuki, L. Ramoino, A. Baratoff, and T. A. Junga, "Molecular Assembly and Self-Assembly: Molecular Nanoscience for Future Technologies", Annals of the New York Academy of Sciences, Vol. 1006, No. Molecular Electronics III, pp. 291–305, 2003.

4. Jain, K. K., "Nanotechnology-based drug delivery for cancer.", Technology in cancer research & treatment, Vol. 4, No. 4, pp. 407, 2005.

5. Huang, X., I. H. El-Sayed, W. Qian, and M. A. El-Sayed, "Cancer cells assemble and align gold nanorods conjugated to antibodies to produce highly enhanced, sharp, and polarized surface Raman spectra: A potential cancer diagnostic marker", Nano Lett, Vol. 7, No. 6, pp. 1591–1597, 2007.

6. Paciotti, G. F., L. Myer, D. Weinreich, D. Goia, N. Pavel, R. E. McLaughlin, and L. Tamarkin, "Colloidal gold: a novel nanoparticle vector for tumor directed drug delivery", Drug Delivery, Vol. 11, No. 3, pp. 169–183, 2004.

7. Wu, X., H. Liu, J. Liu, K. N. Haley, J. A. Treadway, J. P. Larson, N. Ge, F. Peale, and M. P. Bruchez, "Immunofluorescent labeling of cancer marker Her2 and other cellular targets with semiconductor quantum dots", Nature biotechnology, Vol. 21, No. 1, pp. 41–46, 2002.

8. Cohen, M. S., J. M. Stern, A. J. Vanni, R. S. Kelley, E. Baumgart, D. Field, J. A. Libertino and I. C. Summerhayes, "In vitro analysis of a nanocrystalline silver-coated surgical mesh", Surgical Infections, Vol. 8, No. 3, pp. 397–404, 2007.

9. Voskerician, G., M. S. Shive, R. S. Shawgo, H. Recum, J. M. Anderson, M. J. Cima, and R. Langer, "Biocompatibility and biofouling of MEMS drug delivery devices", Biomaterials, Vol. 24, No. 11, pp. 1959–1967, 2003.

10. Yi, H., J. L. Leunissen, G. M. Shi, C. A. Gutekunst, and S. M. Hersch, "A novel procedure for pre-embedding double immunogold-silver labeling at the ultrastructural level", Journal of Histochemistry and Cytochemistry, Vol. 49, No. 3, pp. 279, 2001.

11. Furno, F., K. S. Morley, B. Wong, B. L. Sharp, P. L. Arnold, S. M. Howdle, R. Bayston, P. D. Brown, P. D. Winship, and H. J. Reid, "Silver nanoparticles and polymeric medical devices: a new approach to prevention of infection?", Journal of Antimicrobial Chemotherapy, Vol. 54, No. 6, pp. 1019, 2004.

12. Thomas, M. and A. M. Klibanov, "Conjugation to gold nanoparticles enhances polyethylenimine's transfer of plasmid DNA into mammalian cells", Proceedings of the National Academy of Sciences of the United States of America, Vol. 100, No. 16, pp. 9138, 2003.

13. Chithrani, B. D., A. A. Ghazani, and W. C. Chan, "Determining the size and shape dependence of gold nanoparticle uptake into mammalian cells", Nano Lett, Vol. 6, No. 4, pp. 662–668, 2006.

14. Yen, H. J., S. Hsu, and C. L. Tsai, "Cytotoxicity and immunological response of gold and silver nanoparticles of different sizes", Small, Vol. 5, No. 13, pp. 1553–1561, 2009.

15. Li, J. J., L. Zou, D. Hartono, C. N. Ong, B. H. Bay, and L. Y. Yung, "Gold nanoparticles induce oxidative damage in lung fibroblasts in vitro", Advanced Materials, Vol. 20, No. 1, pp. 138–142, 2008.

16. Hirsch, L. R., R. J. Stafford, J. A. Bankson, S. R. Sershen, B. Rivera, R. E. Price, J. D. Hazle, N. J. Halas, and J. L. West, "Nanoshell-mediated near-infrared thermal therapy of tumors under magnetic resonance guidance", Proceedings of the National Academy of Sciences, Vol. 100, No. 23, pp. 13549, 2003.

17. Carlson, C., S. M. Hussain, A. M. Schrand, L. K. Braydich-Stolle, K. L. Hess, R. L. Jones, and J. J. Schlager, "Unique cellular interaction of silver nanoparticles: size-dependent generation of reactive oxygen species", J. Phys. Chem. B, Vol. 112, No. 43, pp. 13608–13619, 2008.

18. Kawata, K., M. Osawa, and S. Okabe, "In Vitro toxicity of silver nanoparticles at noncytotoxic doses to HepG2 human hepatoma cells", Environ. Sci. Technol, Vol. 43, No. 15, pp. 6046–6051, 2009.

19. Ahamed, M., M. Karns, M. Goodson, J. Rowe, S. M. Hussain, J. J. Schlager, and Y. Hong, "DNA damage response to different surface chemistry of silver nanoparticles in mammalian cells", Toxicology and applied pharmacology, Vol. 233, No. 3, pp. 404–410, 2008.

20. Nadworny, P. L., J. F. Wang, E. E. Tredget, and R. E. Burrell, "Anti-inflammatory activity of nanocrystalline silver in a porcine contact dermatitis model", Nanomedicine: Nanotechnology, Biology and Medicine, Vol. 4, No. 3, pp. 241–251, 2008.

21. Kahraman, M., M. M. Yazici, F. Şahin, and M. Çulha, "Experimental parameters influencing surface-enhanced Raman scattering of bacteria", Journal of Biomedical Optics, Vol. 12, pp. 054015, 2007.

22. Çulha, M., A. Adigüzel, M. M. Yazici, M. Kahraman, F. Şahin, and M. Güllüce, "Characterization of Thermophilic Bacteria Using Surface-Enhanced Raman Scattering", Applied spectroscopy, Vol. 62, No. 11, pp. 1226–1232, 2008.

23. Kahraman, M., M. M. Yazici, F. Sahin, O. F. Bayrak, and M. Çulha, "Reproducible surface-enhanced Raman scattering spectra of bacteria on aggregated silver nanoparticles", Applied spectroscopy, Vol. 61, No. 5, pp. 479–485, 2007.

24. Kamei, H., T. Koide, T. Kojima, Y. Hashimoto, and M. Hasegawa, "Effect of gold on survival of tumor-bearing mice.", Cancer biotherapy & radiopharmaceuticals, Vol. 13, No. 5, pp. 403, 1998.

25. Maier, S. A., Plasmonics: fundamentals and applications, Springer Verlag, 2007

26. Dragoman, M. and D. Dragoman, "Plasmonics: Applications to nanoscale terahertz and optical devices", Progress in Quantum Electronics, Vol. 32, No. 1, pp. 1–41, 2008.

27. Willets, K. A. and R. P. Van Duyne, "Localized surface plasmon resonance spectroscopy and sensing", 2007.

28. Lin, T. J., K. T. Huang, and C. Y. Liu, "Determination of organophosphorous pesticides by a novel biosensor based on localized surface plasmon resonance", Biosensors and Bioelectronics, Vol. 22, No. 4, pp. 513–518, 2006.

29. El-Sayed, I. H., X. Huang, and M. A. El-Sayed, "Surface plasmon resonance scattering and absorption of anti-EGFR antibody conjugated gold nanoparticles in cancer diagnostics: applications in oral cancer", Nano Lett, Vol. 5, No. 5, pp. 829–834, 2005.

30. El-Sayed, I. H., X. Huang, and M. A. El-Sayed, "Selective laser photo-thermal therapy of epithelial carcinoma using anti-EGFR antibody conjugated gold nanoparticles", Cancer letters, Vol. 239, No. 1, pp. 129–135, 2006.

31. Huff, T. B., M. N. Hansen, Y. Zhao, J. X. Cheng, and A. Wei, "Controlling the cellular uptake of gold nanorods", Langmuir, Vol. 23, No. 4, pp. 1596–1599, 2007.

32. Braydich-Stolle, L., S. Hussain, J. J. Schlager, and M. C. Hofmann, "In vitro cytotoxicity of nanoparticles in mammalian germline stem cells", Toxicological Sciences, Vol. 88, No. 2, pp. 412, 2005.

33. Möhlen, K. H. and F. K. Beller, "Use of radioactive gold in the treatment of pleural effusions caused by metastatic cancer", Journal of Cancer Research and Clinical Oncology, Vol. 94, No. 1, pp. 81–85, 1979.

34. Rosenberg, S. J., S. A. Loening, C. E. Hawtrey, A. S. Narayana, and D. A. Culp, "Radical prostatectomy with adjuvant radioactive gold for prostatic cancer: a preliminary report", The Journal of urology, Vol. 133, No. 2, pp. 225–227, 1985.

35. Shukla, R., V. Bansal, M. Chaudhary, A. Basu, R. R. Bhonde, and M. Sastry, "Biocompatibility of gold nanoparticles and their endocytotic fate inside the cellular compartment: a microscopic overview", Langmuir, Vol. 21, No. 23, pp. 10644–10654, 2005.

36. Gao, H., W. Shi, and L. B. Freund, "Mechanics of receptor-mediated endocytosis", Proceedings of the National Academy of Sciences of the United States of America, Vol. 102, No. 27, pp. 9469, 2005.

37. Pan, Z., W. Lee, L. Slutsky, R. A. Clark, N. Pernodet, and M. H. Rafailovich, "Adverse effects of titanium dioxide nanoparticles on human dermal fibroblasts and how to protect cells", Small, Vol. 5, No. 4, pp. 511–520, 2009.

38. Pernodet, N., X. Fang, Y. Sun, A. Bakhtina, A. Ramakrishnan, J. Sokolov, A. Ulman, and M. Rafailovich, "Adverse effects of citrate/gold nanoparticles on human dermal fibroblasts", Small, Vol. 2, No. 6, pp. 766–773, 2006.

39. Stein, G. S. and A. B. Pardee, Cell cycle and growth control: biomolecular regulation and cancer, Wiley-Blackwell, 2004

40. Food, N., "The Prevention of Cancer: a Global Perspective (1997). World Cancer Research Fund", American Association for Cancer Research,

41. Kunal, B., D. Maria, B. Jens, S. Roel, H. Eik, and D. Elke, "Titanium dioxide nanoparticles induce oxidative stress and DNA-adduct formation but not DNA-breakage in human lung cells", Particle and Fibre Toxicology, Vol. 6,

42. Chiara, U., B. Daniele, L. Giada, H. M. Iris, P. Christine, B. Giovanni, U. Ronald, and K. C. James, "Gold nanoparticles induce cytotoxicity in the alveolar type-II cell lines A549 and NCIH441", Particle and Fibre Toxicology, Vol. 6,

43. Foldbjerg, R., D. A. Dang, and H. Autrup, "Cytotoxicity and genotoxicity of silver nanoparticles in the human lung cancer cell line, A549", Archives of Toxicology, pp. 1–8,

44. Berridge, M. V. and A. S. Tan, "Characterization of the cellular reduction of 3-(4, 5-dimethylthiazol-2-yl)-2, 5-diphenyltetrazolium bromide (MTT): subcellular localization, substrate dependence, and involvement of mitochondrial electron transport in MTT reduction", Archives of biochemistry and biophysics, Vol. 303, No. 2, pp. 474–482, 1993.

45. Patra, H. K., S. Banerjee, U. Chaudhuri, P. Lahiri, and A. K. Dasgupta, "Cell selective response to gold nanoparticles", Nanomedicine: Nanotechnology, Biology and Medicine, Vol. 3, No. 2, pp. 111–119, 2007.

46. Danielsen, P. H., S. Loft, and P. Moller, "DNA damage and cytotoxicity in type II lung epithelial (A549) cell cultures after exposure to diesel exhaust and urban street particles", Part Fibre Toxicol, Vol. 5, No. 6, pp. 1743–8977, 2008.

47. Al-Baker, E. A., M. Oshin, C. J. Hutchison, and I. R. Kill, "Analysis of UV-induced damage and repair in young and senescent human dermal fibroblasts using the comet assay", Mechanisms of ageing and development, Vol. 126, No. 6-7, pp. 664–672, 2005.

48. Karlsson, H. L., P. Cronholm, J. Gustafsson, and L. Möller, "Copper oxide nanoparticles are highly toxic: a comparison between metal oxide nanoparticles and carbon nanotubes", Chem. Res. Toxicol, Vol. 21, No. 9, pp. 1726–1732, 2008.

49. Kang, S. J., B. M. Kim, Y. J. Lee, and H. W. Chung, "Titanium dioxide nanoparticles trigger p53-mediated damage response in peripheral blood lymphocytes", Environmental and molecular mutagenesis, Vol. 49, No. 5, pp. 399–405, 2008.

50. Mroz, P., A. Pawlak, M. Satti, H. Lee, T. Wharton, H. Gali, T. Sarna, and M. R. Hamblin, "Functionalized fullerenes mediate photodynamic killing of cancer cells: Type I versus Type II photochemical mechanism", Free Radical Biology and Medicine, Vol. 43, No. 5, pp. 711–719, 2007.

51. Colognato, R., A. Bonelli, J. Ponti, M. Farina, E. Bergamaschi, E. Sabbioni, and L. Migliore, "Comparative genotoxicity of cobalt nanoparticles and ions on human peripheral leukocytes in vitro", Mutagenesis, Vol. 23, No. 5, pp. 377, 2008.

52. Gasparyan, V. K., "Gold and silver nanoparticles in bioassay, cell visualization and therapy", Current Clinical Pharmacology, Vol. 4, No. 2, pp. 159–163, 2009.

53. Auffan, M., J. Rose, T. Orsiere, M. De Meo, A. Thill, O. Zeyons, O. Proux, A. Masion, P. Chaurand, O. Spalla, and others, "CeO2 nanoparticles induce DNA damage towards human dermal fibroblasts in vitro", Nanotoxicology, Vol. 3, No. 2, pp. 161–171, 2009.

54. Henson, P. M., D. L. Bratton, and V. A. Fadok, "Apoptotic cell removal", Current Biology, Vol. 11, No. 19, pp. R795–R805, 2001.

55. Alberts, B., D. Bray, A. Johnson, J. Lewis, M. Raff, K. Roberts, P. Walter, and A. M. Campbell, Essential cell biology, Garland Science New York, 2004

56. Pan, Y., A. Leifert, D. Ruau, S. Neuss, J. Bornemann, G. Schmid, W. Brandau, U. Simon, and W. Jahnen-Dechent, "Gold nanoparticles of diameter 1.4 nm trigger necrosis by oxidative stress and mitochondrial damage", Small, Vol. 5, No. 18, pp. 2067–2076, 2009.

57. Kang, B., M. A. Mackey, and M. A. El-Sayed, "Nuclear Targeting of Gold Nanoparticles in Cancer Cells Induces DNA Damage, Causing Cytokinesis Arrest and Apoptosis", J. Am. Chem. Soc, Vol. 132, No. 5, pp. 1517–1519, 2010.

58. Wright, J. B., K. Lam, A. G. Buret, M. E. Olson, and R. E. Burrell, "Early healing events in a porcine model of contaminated wounds: effects of nanocrystalline silver on matrix metalloproteinases, cell apoptosis, and healing", Wound Repair and Regeneration, Vol. 10, No. 3, pp. 141–151, 2002.

59. Hsin, Y. H., C. F. Chen, S. Huang, T. S. Shih, P. S. Lai, and P. J. Chueh, "The apoptotic effect of nanosilver is mediated by a ROS-and JNK-dependent mechanism involving the mitochondrial pathway in NIH3T3 cells", Toxicology letters, Vol. 179, No. 3, pp. 130–139, 2008.

60. Jin, C. Y., B. S. Zhu, X. F. Wang, and Q. H. Lu, "Cytotoxicity of titanium dioxide nanoparticles in mouse fibroblast cells", Chem. Res. Toxicol, Vol. 21, No. 9, pp. 1871–1877, 2008.

61. Levine, A. J., "p53, the cellular gatekeeper for growth and division.", Cell, Vol. 88, No. 3, pp. 323, 1997.

62. Roth, J. A., S. G. Swisher, R. E. Meyn, and others, "p53 tumor suppressor gene therapy for cancer", Oncology-Huntington, Vol. 13, No. 5, pp. 148–154, 1999.

63. Clifford, B., M. Beljin, G. R. Stark, and W. R. Taylor, "G2 arrest in response to topoisomerase II inhibitors: the role of p53", Cancer research, Vol. 63, No. 14, pp. 4074, 2003.

64. Sherr, C. J., "Principles of tumor suppression", Cell, Vol. 116, No. 2, pp. 235–246, 2004.

65. Martins, C. P., L. Brown-Swigart, and G. I. Evan, "Modeling the therapeutic efficacy of p53 restoration in tumors", Cell, Vol. 127, No. 7, pp. 1323–1334, 2006.

66. Fuster, J. J., S. M. Sanz-González, U. M. Moll, and V. Andrés, "Classic and novel roles of p53: prospects for anticancer therapy", Trends in Molecular Medicine, Vol. 13, No. 5, pp. 192–199, 2007.

67. Marx, J., "Recruiting the cell's own guardian for cancer therapy", Science (Washington), Vol. 315, No. 5816, pp. 1211–1213, 2007.

68. Yu, Q., "Restoring p53-mediated apoptosis in cancer cells: new opportunities for cancer therapy", Drug Resistance Updates, Vol. 9, No. 1-2, pp. 19–25, 2006.

69. Ahamed, M., M. A. Siddiqui, M. J. Akhtar, I. Ahmad, A. B. Pant, and H. A. Alhadlaq, "Genotoxic potential of copper oxide nanoparticles in human lung epithelial cells", Biochemical and Biophysical Research Communications, Vol. 396, No. 2, pp. 578-583, 2010.

70. Zhu, L., D. W. Chang, L. Dai, and Y. Hong, "DNA damage induced by multiwalled carbon nanotubes in mouse embryonic stem cells", Nano Lett, Vol. 7, No. 12, pp. 3592–3597, 2007.

71. Asharani, P. V., N. Xinyi, M. P. Hande, and S. Valiyaveettil, "DNA damage and p53-mediated growth arrest in human cells treated with platinum nanoparticles", Nanomedicine, Vol. 5, No. 1, pp. 51–64, 2010.

72. Handley, D. A. and Hayat, M. A, "Colloidal gold: principles, methods, and applications", pp. 12–32, 1989.

73. Martinez-Castanon, G. A., N. Nino-Martinez, F. Martinez-Gutierrez, J. R. Martinez-Mendoza, and F. Ruiz, "Synthesis and antibacterial activity of silver nanoparticles with different sizes", Journal of Nanoparticle Research, Vol. 10, No. 8, pp. 1343–1348, 2008.

74. Lee, P. C. and D. Meisel, "Adsorption and surface-enhanced Raman of dyes on silver and gold sols", The Journal of Physical Chemistry, Vol. 86, No. 17, pp. 3391–3395, 1982.

75. Sur, I., D. Cam, M. Kahraman, A. Baysal, and M. Culha, "Interaction of multi-functional silver nanoparticles with living cells", Nanotechnology, Vol. 21, pp. 175104, 2010.

76. Oliveira, R. J., R. Matuo, A. F. Da Silva, H. J. Matiazi, M. S. Mantovani, and L. R. Ribeiro, "Protective effect of beta-glucan extracted from Saccharomyces cerevisiae, against DNA damage and cytotoxicity in wild-type (k1) and repair-deficient (xrs5) CHO cells", Toxicology in Vitro, Vol. 21, No. 1, pp. 41–52, 2007.

77. Saunders, D. E., W. D. Lawrence, C. Christensen, N. L. Wappler, H. Ruan, and G. Deppe, "Paclitaxel-induced apoptosis in MCF-7 breast-cancer cells", International journal of cancer, Vol. 70, No. 2, pp. 214–220, 1997.

78. Fajao, A., J. Da Silva, J. C. Ahomadegbe, J. G. Rateau, J. F. Bernaudin, G. Riou, and J. Bénard, "Cisplatin-induced apoptosis and p53 gene status in a cisplatin-resistant human ovarian carcinoma cell line", International Journal of Cancer, Vol. 68, No. 1, pp. 67–74, 1996.